МІНІСТЕРСТВО ОСВІТИ І НАУКИ УКРАЇНИ

НАЦІОНАЛЬНИЙ УНІВЕРСИТЕТ «ЗАПОРІЗЬКА ПОЛІТЕХНІКА»

Електротехнічний факультет

(повне найменування факультету)

Електричні та електронні апарати

(повне найменування кафедри)

Пояснювальна записка

до магістерської роботи

магістр

(ступінь вищої освіти)

на тему: Дослідження та розробка електромагнітного приводу контактора змінного струму 380 В, 80 А

(назва теми)

Виконав(ла): студент(ка) ІІ курсу, групи Е-413ам

Спеціальності 141 Електроенергетика,
(код і найменування спеціальності)
електротехніка та електромеханіка

Освітня програма (спеціалізація)
«Електричні та електронні апарати»

БОНДАРЕНКО А.О.
(ПРІЗВИЩЕ та ініціали)

Керівник БЛИЗНЯКОВ О.В.
(ПРІЗВИЩЕ та ініціали)

Рецензент САХНО О.А.

2024

МІНІСТЕРСТВО ОСВІТИ І НАУКИ УКРАЇНИ

Національний університет «Запорізька політехніка»

Факультет *Електротехнічний*
Кафедра Електричні та електронні апарати
Спеціальність 141 Електроенергетика, електротехніка та електромеханіка
(назва освітньої програми (спеціалізації)

ЗАТВЕРДЖУЮ
Завідувач кафедри _____

«_____» _____2024 року

З А В Д А Н Н Я

НА МАГІСТЕРСЬКУ РОБОТУ СТУДЕНТА

Бондаренко Андрій Олегович
(ПРІЗВИЩЕ, ім'я, по батькові)

1. Тема проєкту (роботи): Дослідження та розробка електромагнітного приводу контактора змінного струму 380 В, 80 А
керівник роботи: к.т.н., доц. БЛИЗНЯКОВ Олександр Вікторович
(науковий ступінь, вчене звання, ПРІЗВИЩЕ, ім'я, по батькові)

затверджені наказом ректора НУ «Запорізька політехніка» від «20» листопада

2024 року № 481

2. Строк подання студентом проєкту (роботи) 9.12.2024 р.

Вихідні данні до проєкту (роботи): *Номінальний робочий струм 80 А; номінальна напруга 380 V, головні контакти: 3 замильні; допоміжні контакти: 1замикальний, 1розмикальний; комутаційна зносостійкість – 10^6циклів вмикання-вимикання; напруга живлення електромагнітного приводу – 380 В*

4. ЗМІСТ розрахунково–пояснювальної записки (перелік питань, що їх належить розробити): *Вступ. 1 Техніко-економічне обґрунтування проекту. 2 Розрахунок струмоведучих елементів контуру. 3 Конструювання механізму апарату. 4 Попередній розрахунок електромагніту. 5 Розрахунок системи дугогасіння. 6 Розрахунок пружин. 7. Моделювання у програмному середовищі FEMM*

5. Перелік графічного матеріалу (з точним визначенням обов'язкових креслень): *1) Загальний вигляд контактора; 2) Електромагнітний привод; 3) Система головних контактів; 4) Система допоміжних контактів; 5)–8) Робочі креслення деталей та плакати*

6. Консультанти розділів проєкту (роботи)

Розділ	ПРІЗВИЩЕ, ініціали та посада консультанта	Підпис, дата	
		завдання видав	прийняв виконане завдання
1-8	БЛИЗНЯКОВ О.В., доцент		

7. Дата видачі завдання «__27__» _____вересня_____ 2024 року.

КАЛЕНДАРНИЙ ПЛАН

№ з/п	Назва етапів курсового проєкту (роботи)	Строк виконання етапів проєкту (роботи)	Примітка
1	Огляд дизайну, вибір аналога	1 тиждень	
2	Розрахунок струмоведучих елементів контуру	2-3	
3	Конструювання механізму апарату	4	
4	Попередній розрахунок електромагніту	5	
5	Розрахунок системи регулювання дуги, розрахунок пружин	6	
6	Виконання креслень	7-8	
7	Оформлення пояснювальної записки	9	

Студент(ка) _____ Бондаренко А.О.
(підпис) (Ім'я ПРІЗВИЩЕ)

Керівник проєкту (роботи) _____ Близняков О.В
(підпис) (Ім'я ПРІЗВИЩЕ)

РЕФЕРАТ

ПЗ: 79 стор., 1 табл., 25 рис., 32 джерела.

КОНТАКТОР ЗМІННОГО СТРУМУ, МАГНІТНИЙ ПУСКАЧ, СТРУМОВЕДУЧИЙ КОНТУР, ШИНИ, КОМУТАЦІЙНІ КОНТАКТИ, ТЕМПЕРАТУРА, ПРУЖИНА, ЕЛЕКТРОМАГНІТ, ЗАХИСТ ВІД ПЕРЕВАНТАЖЕННЯ

Об’єкт дослідження – електромагнітний привод контактора змінного струму на 80 А та 380 В.

Мета роботи – дослідження та оптимізація електромагнітного приводу контактора змінного струму, розрахованого на 80 А та 380 В.

Методи дослідження – в роботі використовувалися різні методи дослідження, включаючи ретельний аналіз технічної літератури, промислових стандартів, комплексні розрахунки для різних умов експлуатації. Методами проектування, що використовуються, є дослідження та постійне вдосконалення з використанням процедури розрахунку, рекомендованої експертами в цій галузі [18].

Результати дослідження чітко показують, що ця контакторна система є ефективною та надійною, тому це найкраще рішення для запуску та керування двигунами. Конструкція захищає двигун не тільки від перевантажень, але і від поломок, для стабільної та безпечної роботи.

ABSTRACT

EN: p. 79, 6 tab., 25 fig., 32 sources.

ALTERNATING CURRENT CONTACTOR, MAGNETIC STARTER, CURRENT-CARRYING CIRCUIT, BUSES, SWITCHING CONTACTS, TEMPERATURE, SPRING, ELECTROMAGNET, OVERLOAD PROTECTION.

The object of the study is an electromagnetic drive of an AC contactor rated at 80 A and 380 V.

The aim of the work is to study and optimize an electromagnetic drive of an AC contactor rated at 80 A and 380 V.

Research methods – various research methods were used in the work, including a thorough analysis of technical literature, industrial standards, and complex calculations for different operating conditions. The design methods used are research and continuous improvement using a calculation procedure recommended by experts in this field [18].

The results of the study show clearly that this contactor system is efficient and reliable so it’s the best solution for starting and controlling motors. The design protects the motor not only from overloads but also from failures, for stable and safe operation.

CONTENTS

РЕФЕРАТ 3
ABSTRACT 4
INTRODUCTION 6
1 FEASIBILITY STUDY OF THE PROJECT 7
1.1 Design overview 7
1.2 Consideration of important aspects of an electrical device 8
1.3 Review of existing models. 10
1.4 Choice of analogue. 14
1.5 Detailed description of analogue. 176
2 CALCULATION OF CURRENT-CARRYING CIRCUIT ELEMENTS 198
2.1 Calculation of output buses 209
2.2 Contact connections 22
2.3 Switching contacts 276
2.4 Calculation of wearing and follow through of contacts 31
3 DESIGNING OF APPARATUS MECHANISM 34
4 PRELIMINARY CALCULATION OF ELECTROMAGNET 388
5 CALCULATION OF ARC CONTROL SYSTEM 45
6 THE CALCULATION OF SPRINGS 499
6.1 The calculation of contact spring 499
6.2 The calculation of opposing spring 51
7 MODELING IN THE FEMM PROGRAM 549
7.1 Description of the FEMM program 549
7.2 Building a model of an AC electromagnet 59
7.3 Creating a Model of an AC electromagnet, parameter output 66
CONCLUSION 80
LIST OF REFERENCES 81

INTRODUCTION

The contactor is an apparatus of mass application, produced in large quantities and widely used, therefore the task is always to simplify the design, improve the technology, which is what this project is dedicated to.

Contactors play a pivotal role in industrial settings, where they are utilized to regulate and oversee electrical loads spanning a diverse array of applications. Whether it entails the control of motors, illumination systems, heating mechanisms, or even the management of capacitor banks and thermal evaporators, contactors serve as a dependable means of operation. They are available in varying dimensions, ranging from compact handheld devices to larger units that occupy substantial space. It is noteworthy to acknowledge that contactors possess distinct characteristics that set them apart from circuit breakers, as their primary purpose does not involve the interruption of short circuit currents. Nonetheless, they bestow an additional advantage by acting as a safeguard against voltage drops within the network, thereby ensuring a steadfast and unwavering power supply.

In addition to breaking during normal operations, electromagnetic contactors can also serve as protection against voltage drops in the network. As the voltage drops and the electromagnet can no longer maintain the contactor in the moving system, it is spontaneously switched off.

This project centers around the calculation and meticulous design of an AC contactor, specifically engineered to handle a rated current of 80 A and a rated voltage of 380 V. Its primary objective is to enhance the technical functionalities of contactors, ensuring heightened efficiency, reliability, and adaptability to a wide array of motor initiation and deceleration requirements. Furthermore, the project places considerable emphasis on optimizing economic factors, encompassing the reduction of power losses, enhancement of energy efficiency, and strategic integration of cost-effective manufacturing methodologies. By pursuing these objectives, this endeavor aims to revolutionize the capabilities and performance of contactors, fostering advancements in the field of electrical engineering.

1 FEASIBILITY STUDY OF THE PROJECT

1.1 Design overview

The contactor, a widely utilized device in industrial applications, undergoes constant refinement to simplify its design and enhance its technological capabilities, which is the primary focus of this project.

Contactor technology plays a crucial role in industrial environments, where it manages electrical loads across various applications such as motor control, lighting systems, heating elements, and the regulation of capacitor banks and thermal evaporators. Available in a range of sizes, from compact handheld models to larger units, contactors distinguish themselves from circuit breakers by not primarily interrupting short circuit currents. However, they provide an added layer of security by preventing voltage drops within the system, ensuring a consistent power supply.

Moreover, electromagnetic contactors not only break circuits during normal operations but also protect against voltage drops in the network. When voltage decreases and the electromagnet can no longer sustain the contactor's position within the system, it automatically switches off.

This project specifically focuses on designing an AC contactor capable of handling a rated current of 80 A and a rated voltage of 380 V. Its aim is to improve the technical aspects of contactors, enhancing efficiency, reliability, and adaptability to various motor start-up and deceleration requirements. Additionally, the project emphasizes optimizing economic factors such as reducing power losses, improving energy efficiency, and incorporating cost-effective manufacturing methods. By pursuing these goals, the project seeks to advance contactor capabilities and performance, driving innovation in electrical engineering.

Furthermore, this project will investigate the development of the contactor with a focus on studying magnetic fields, their influence on device characteristics, and the reciprocal impact of magnetic fields on the overall electrical apparatus.

1.2 Consideration of important aspects of an electrical device

Before considering analogues, it is worth looking at some features that you should pay attention to before choosing an electrical device.

The primary functions of AC contactors revolve around the frequent switching of high-current main circuits, a necessity particularly prevalent within low-voltage control systems [1].

It's essential to acknowledge the profound impact of vibration environments on the degradation of AC contactor performance. The service life of these components intricately intertwines with their dynamic characteristics during operation. When the closing process occurs, vibration stress can modify the impact energy of the iron core, potentially disrupting the dynamic response characteristics of the contact. This alteration may consequently impinge upon the operational performance and overall longevity of AC contactors.

Employing the finite element method enables the calculation of dynamic characteristics. By meticulously analyzing factors such as armature and magnetic ring parameters within Maxwell's transient magnetic field model, one can strive towards achieving an optimal electromagnetic field design. Additionally, it's imperative to address contact bounce during the closing process, as it stands as a critical factor influencing contact wear and the electrical life of the device. Excessive energy stemming from electromagnetic mechanism core collisions may give rise to secondary bounces, thereby instigating contact abrasion and significantly diminishing the electrical contactor's lifespan. The coil closing phase angle during AC contactor operation closely correlates with the closing process.

Research in [2] indicates that under low-acceleration vibration, dynamic characteristic variations are smaller, with less impact on electromagnetic mechanisms. Vibration frequency influences actuation time and contact performance, with lower frequencies affecting actuation time more significantly and higher frequencies impacting contact performance to a greater extent.

Moreover, a detailed virtual prototype model is presented in [3], enabling simulation of dynamic processes and contact bounce using communication circuit, electromagnetic field, and mechanical motion equations.

Article [4] introduces a switch model capable of adjusting both magnetic and contact gaps of AC contactors.

The residual electrical endurance of AC contactors, as discussed in [5], reflects their line on-off performance. Timely prediction of this endurance before failure can markedly enhance power system reliability and reduce economic losses.

Given the significance of AC contactors to power systems, researchers have conducted extensive studies on predicting residual-electrical-endurance in recent years. For example, M. Zong et al. addressed voltage switching challenges for AC-3 and AC-4 operating conditions in [6], enhancing test accuracy using PLC and a new transformer setup. In [7], Z. Wu et al. proposed a modeling method based on conditional density estimation for accurate residual-electrical-endurance prediction. S. Kumari et al. estimated AC contactors' health status in [8] by examining feature parameters such as contact resistance and residual-electrical-endurance. Additionally, control strategies were investigated by Z. Wu et al. in [9] to improve AC contactors' electrical life by studying the relationship between arc phase angle, arc energy, and contact mass loss. Simulation of electrical-endurance distribution characteristics based on a contact ablation model was conducted by S. Zheng et al. in [10], along with reliability evaluation through electrical endurance tests. H. Cui et al. utilized a convolutional neural network (CNN) in [11] to construct an electrical-endurance-prediction model, extracting voltage and current waveform signals and employing a voting mechanism for enhanced prediction accuracy.

Similarly, S. Sun et al. utilized Euclidean distance calculations and statistical indicator correlations in [12] for residual-electrical-endurance prediction using a one-dimensional regression model. In [13], K. Li et al. established a Wiener degradation model with normally distributed degradation variables, validated through simulated residual-electrical-endurance tests using the Monte Carlo method. Finally, S. Abirami et al. developed a stochastic gradient-descent classifier model in

[14] for estimating residual-electrical-endurance prediction using operational data across different operating conditions.

However, certain critical aspects were overlooked in the aforementioned investigations concerning the prediction of residual-electrical-endurance of AC contactors: (1) Limited adoption of feature parameters hindered effective representation of degradation information, thereby impacting prediction accuracy. (3) The electrical endurance of AC contactors was not considered as a long time-series problem, neglecting the importance of considering both current and previous states in determining residual-electrical-endurance and underutilizing the relationship between pre- and post-degradation states, thus limiting precision.

In conclusion, it is imperative to carefully consider the comprehensive information provided when making a selection among analogues for AC contactors. This text sheds light on several critical aspects, such as the fundamental functions of AC contactors, the impact of vibration environments on performance degradation, and the importance of accurately predicting residual-electrical-endurance to bolster power system reliability. Furthermore, the discourse delves into extensive research endeavors aimed at comprehending and enhancing the performance and longevity of AC contactors, spanning from intricate analyses of dynamic characteristics to the development of sophisticated prediction models.

1.3 Review of existing models

To streamline the work process and gain a deeper understanding of the topic, it is essential to explore existing analogues. By analyzing similar systems or components, we can identify proven solutions, recognize potential challenges, and apply best practices to our current application. This comparative analysis not only simplifies the design or implementation phase but also helps in predicting system behavior under different conditions. Moreover, studying existing analogues provides insights into performance optimization, reliability enhancements, and cost-effective

approaches, which are crucial for ensuring long-term efficiency and safety in electrical systems.

There are a lot of different contactors and magnetic starters with rated parameters 80 A and 380 V. The device is shown on the KT series contactor, figure 1.1 [30]

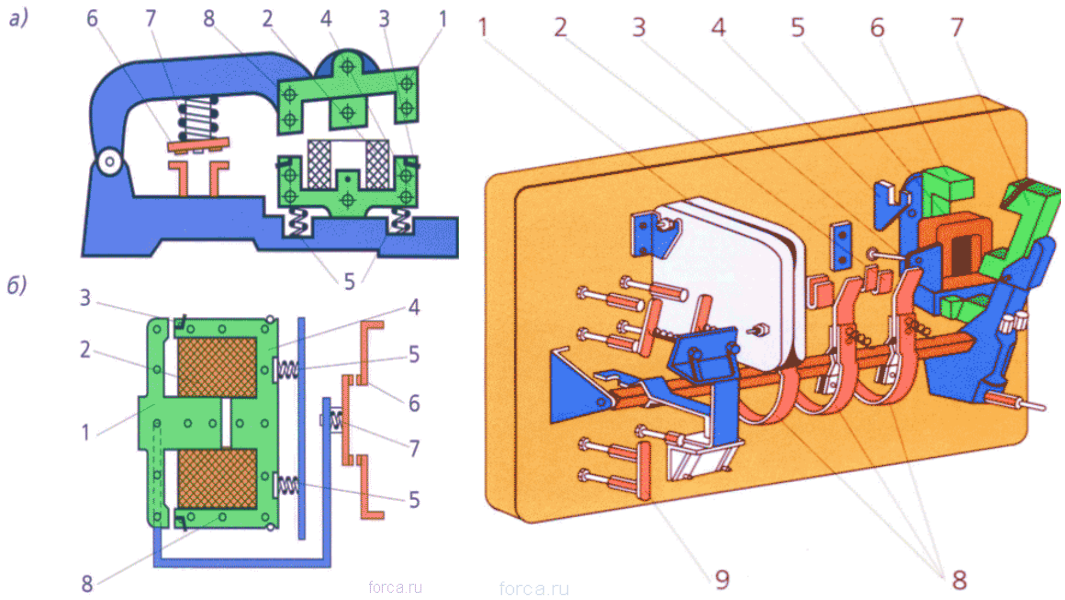

a – AC contactor system: 1 – anchor; 2 – coil; 3 – shading ring; 4 – magnetic core; 5 – shock-absorbing springs; 6 – contacts; 7 – opposing spring; 8 – tie rods; b – the whole AC contactor construction: 1 – arc chute; 2 – fixed contact; 3 – movable contact; 4 - camera mounting bracket (bail); 5 – coil; 6 – core; 7 – anchor; 8 – flexible electric connection; 9 – interlocking contacts.

Figure 1.1 - General view of AC contactors and their main components

Import analogues of AC contactors can also be found in the production lines of SEZ and Siemens. SEZ power contactors are widely utilized in both industrial applications and everyday environments, covering a current range from 9 A to 90 A. These contactors are known for their reliability and versatility, making them suitable for controlling motors, lighting systems, and various electrical loads.

Siemens, being a global leader in electrical engineering, offers a comprehensive range of contactors designed for higher performance, durability, and advanced control features, making their products ideal for demanding industrial applications. The availability of these imported options provides flexibility in selecting the most suitable contactor based on specific operational requirements. The picture, that helps to understand the consctuction is shown in figure 1.2 [28]

Figure 1.2 - SEZ CNN 40 00 18,5kW 400V, 50A, AC

Siemens provides a diverse selection of contactors tailored to meet a broad spectrum of applications, including pre-assembled contactor assemblies. These devices are highly regarded for their outstanding contact reliability, long operational life, and ability to maintain performance even in challenging environmental conditions. Such qualities make Siemens contactors an ideal choice for customers seeking durable and dependable solutions for their electrical systems. Whether in industrial automation, power distribution, or motor control, Siemens contactors consistently deliver the reliability and efficiency needed to ensure smooth and safe operation in a wide variety of settings. Figure 1.3 is taken from [29].

Figure 1.3 - SIEMENS 3RT2026-1AP00 400V, 25A, AC

Noark Electric, as part of the Chinese Chint Group, one of the world's largest manufacturers of electrical equipment, produces a wide range of reliable and efficient electrical devices that meet high quality and safety standards. Among their product lineup, Noark contactors stand out for their robust design, durability, and adherence to international standards such as IEC.

Noark contactors are specifically designed for both industrial and commercial applications, ensuring reliable operation in various electrical circuits. They are used for controlling and switching motors, lighting systems, and other electrical loads. The contactors are engineered to handle demanding environments, offering a combination of high switching capacity, long mechanical life, and energy efficiency. These features make Noark contactors a dependable solution for users seeking quality and performance in power control and automation systems.

Figure 1.4 – NOARK Ex9C80 11 3P 400V 80A, AC

1.4 Choice of analogue

Following a review of both domestic and foreign alternatives, the ПМ 4-80 contactor was selected. This contactor is an electromagnetic device designed for the remote and frequent switching of AC and DC power circuits. It offers a reliable and safe method for controlling heavy-load electric motors, ensuring efficient operation under high-demand conditions.

In addition, when equipped with thermal relays, contactors like the ПМ 4-80 function similarly to magnetic starters, providing not only switching capabilities but also protection against motor overload. This integration helps safeguard motors from damage by disconnecting the circuit if the current exceeds the set threshold, further enhancing the contactor's versatility in industrial applications.

Image of contactor is shown on figures 1.5, 1.6 [27]

Figure 1.5 – The contactor ПМ 4-80

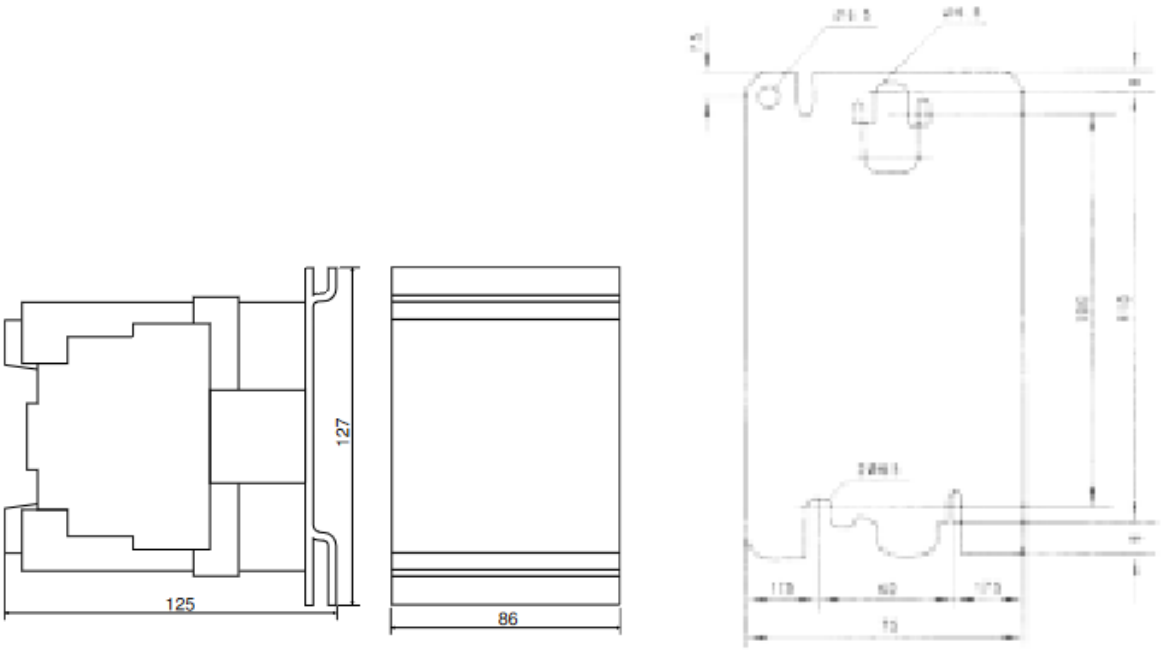

a – overall, mounting dimensions;

b – connecting dimensions.

Figure 1.6 Dimensions of contactors ПМ 4-80

1.5 Detailed description of analogue.

This device is designed for starting, stopping, and reversing asynchronous electric motors with a squirrel-cage rotor, as well as controlling various types of resistive and inductive loads. Its versatile mounting options allow it to be installed either on a mounting plate or a DIN rail, making it adaptable to different electrical setups and configurations. This flexibility ensures that the contactor can be easily integrated into a wide range of industrial and commercial applications, providing reliable and efficient control over electrical loads and motor operations.

The apparatus is called ПМ 4-80 on 380 V, where:

- mode of operation: Long-term;
- volume, kg: 0.00117;
- nominal operating current I_n, A: 80;
- nominal operating voltage U_n, V: AC 380;
- application category: AC-3, AC-4;
- type of additional contacts: 1NO+1NC;
- degree of protection: IP20;
- weight, kg: 1.46;
- type of contacts: 3NO;

Climatic peculiarities of contactor operation:

- ambient temperature -15…+45 °C;
- precipitation (contactor can withstand hoarfrost fall and its melting in off-state);
- relative humidity less than 98% at ambient temperature not more than 40 °C;
- mechanical loads.

The ПМ 4-80 contactor is designed for fixed installations to remotely control the starting, stopping, and reversing of asynchronous motors with squirrel-cage rotors at AC voltages up to 660 V and frequencies of 50 Hz or 60 Hz. This contactor is ideally suited for use in industrial applications where motors are directly connected to a 380V network. It offers a reliable solution for managing heavy-load

equipment through efficient motor control, ensuring smooth operation even in demanding conditions.

One of the key advantages of this device is its compatibility with microprocessor-based control systems, making it highly versatile in modern automation environments. It supports coil bridging with interference suppression devices, enhancing its resistance to electrical noise, which is particularly beneficial when using thyristor-based control systems or other sensitive electronics.

Additionally, the ПМ 4-80 contactor is valued for its compact size, cost-effectiveness, and ease of installation and use. The device features adjustable parameters, which allow for fine-tuning of its operation to meet the specific needs of various projects. These characteristics make it an optimal choice for constructing and configuring electrical apparatus, ensuring both performance and adaptability within the given technical specifications.

In summary, the ПМ 4-80 offers a robust and affordable solution for controlling motors in industrial settings, while its compatibility with advanced control systems and interference suppression capabilities make it an excellent choice for high-performance automation systems.

2 CALCULATION OF CURRENT-CARRYING CIRCUIT ELEMENTS

Initial data for calculation and designing of current-carrying circuit:

- rated voltage U_n is 380 V;
- rated current I_n is 80 A;
- maximal breaking current I_{br} is 6 I_n A;
- tripping frequency per hour Z is 1200 tripping/hour;
- switching life N_{el} is 1 millions of cycles.

The objective of the calculation is to determine the appropriate cross-sectional dimensions of the current-carrying circuit, assess the resistance of the materials used, analyze transitional resistance at contact connections, estimate voltage drops across the circuit, and evaluate both thermal and dynamic resistance. Maintaining the temperature of the components within safe limits is essential to ensure reliability and longevity in operation.

Furthermore, the calculation seeks to confirm that the pressure exerted by the switching contacts is sufficient to prevent welding or inadvertent disconnections due to electro-dynamic forces. This aspect is particularly critical in applications involving high currents or frequent switching operations, where the risk of contact fusion or failure could lead to operational downtime or equipment damage.

By conducting a thorough analysis of these parameters, the calculation ensures that the electrical system operates efficiently and safely under expected load conditions. It also helps in optimizing the design, enhancing the overall performance of the electrical circuit while minimizing the risk of failures and maintaining compliance with relevant safety standards. This comprehensive approach ultimately contributes to the reliability and effectiveness of the electrical system in its intended application.

Current-carrying circuit of alternative current of magnetic starter our type is represented in figure 2.1.

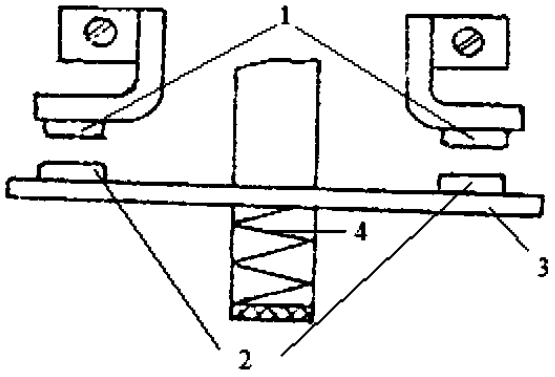

1– fixed contact, 2 – movable contact, 3 – contact plates, 4 – contact spring.

Figure 2.1 – Current-carrying circuit of contactor

Calculation of current-carrying units of apparatus is carried out for two regimes: long-term flowing of rated current I_n and short-time flowing of maximal breaking current I_{br}.

2.1 Calculation of output buses

Dimensions of current-carrying non-insulated conductor are calculated by Newton formula [17; 19]

$$p \cdot q = \frac{{I_n}^2 \cdot \rho_0 \cdot (1+\alpha_c \cdot \vartheta_c) \cdot k_{\text{add\_losses}}}{k_t \cdot (\vartheta_c - \vartheta_{\text{env}})}, \quad (2.1)$$

where p is perimeter of cross section of a conductor, taking part in heat exchange with environment, cm;

S is cross section of conductor, cm;

ρ_0 is specific electrical resistance at 0 ^{0}C; ρ_0 is equal $1.62 \cdot 10^{-6}$ Ohm·cm;

a is temperature coefficient of resistance; a is equal $4.3 \cdot 10^{-3}$ 1/deg;

ϑ_c is long-term admissible temperature of conductor heating (is chosen in accordance with to ГОСТ 403-73); ϑ_c is 105^0C;

K_{ad} is coefficient of additional losses caused by skin and proximity effects; K_{ad}=1;

ϑ_{env} is ambient temperature (usually ϑ_{env} is 40 ^{0}C);

K_T is heat transfer coefficient; K_T is 7 W/cm^2 · deg.

For non-insulated rectangular bus with sides a and b taking into account m = a / b, when pq = 2m(1+m)b^3

$$b = \sqrt[3]{\frac{\left(I_n{}^2 \cdot \rho_0 \cdot k_{add\_losses} \cdot (1+\alpha_c \cdot \vartheta_c)\right)}{2 \cdot m \cdot (m+1) \cdot k_t \cdot (\vartheta_c - \vartheta_{\text{env}})}}, \quad (2.2)$$

where m is ratio between sides of the bus; m is 0.2;

K_{ad} is equal to 1.

$$b = \sqrt[3]{\frac{\left(80^2 \cdot 1.62 \cdot 10^{-6} \cdot 1 \cdot (1 + 4.3 \cdot 10^{-3} \cdot 105)\right)}{2 \cdot 0.2 \cdot (0.2 + 1) \cdot 7 \cdot 10^{-4} \cdot (105 - 40)}} = 0.8833 \text{ cm}.$$

The value of size a can be found from expression m = a / b

$$a = m \cdot b, \quad (2.3)$$

$$a = 0.2 \cdot 0.8833 = 0.1767 \text{ cm}.$$

It is now possible to calculate section of a bus by using following formula:

$$S = a \cdot b, \quad (2.4)$$

$$S = 0.1767 \cdot 0.8833 = 0.156 \text{ cm}^2.$$

According to ГОСТ 434-78 the nearest larger standard cross section of a bus S and standard values of dimensions a and b are chosen

$S = 0.2$ cm^2; a = 0.2 cm; b = 1 cm.

For chosen dimensions of cross section steady-state heating temperature is calculated by formula

$$\vartheta_{\text{set}} = \vartheta_{\text{env}} + \frac{\rho_0 \cdot (1+\alpha_c \cdot \vartheta_c) \cdot I_n{}^2 \cdot k_{\text{add\_losses}}}{k_t \cdot S \cdot p}, \quad (2.5)$$

where p is perimeter of bus cross section, which is calculated by next formula

$$\text{p} = 2 \cdot (\text{a} + \text{b}), \quad (2.6)$$

$$\text{p} = 2 \cdot (0.2 + 1) = 2.4 \text{ cm}.$$

Steady-state heating temperature of a bus (2.5)

$$\vartheta_{\text{set}} = 40 + \frac{1.62 \cdot 10^{-6} \cdot (1+4.3 \cdot 10^{-3} \cdot 105) \cdot 80^2 \cdot 1}{7 \cdot 10^{-4} \cdot 0.2 \cdot 2.4} = 84.7891^0\text{C}.$$

Steady-state heating temperature of a bus ϑ_{set} is 84.7891^0C, that value is less than admissible heating temperature of a bus in long-term regime ϑ_{c} is 105^0C according to ГОСТ 434-70, so it can be concluded that calculation was made correctly.

Obtained bus cross section is verified for thermal stability in maximal breaking current I_{br} flow regime. Estimate the thermal stability of the apparatus. To do this, calculate the parameter $I^2_{br}\, t_{sc}$, called the thermal impulse:

$$A_{\text{th\_s}} = \frac{\gamma \cdot C \cdot S^2 \cdot \ln\left(\frac{1+\alpha_C \cdot \vartheta_{\text{sc}}}{1+\alpha_C \cdot \vartheta_C}\right)}{\rho_0 \cdot \alpha_c \cdot k_{\text{add\_losses}}}, \quad (2.7)$$

$$A_{\text{th\_s}} = \frac{8.94 \cdot 0.39 \cdot 0.2^{\,2} \cdot \ln\left(\frac{1 + 4.3 \cdot 10^{-3} \cdot 300}{1 + 4.3 \cdot 10^{-3} \cdot 105}\right)}{1.62 \cdot 10^{-6} \cdot 4.3 \cdot 10^{-3} \cdot 1} = 9.1285 \cdot 10^6\ A^2 \cdot s.$$

where γ is density of bus material; γ is 8.94 g/cm^3;

C is specific heat capacity; C is 0.39 J/g · deg;

ϑ_{sc} , ϑ_c is admissible heating temperature correspondently of current-carrying bus in short-circuit regime and conductor in long-term regime; ϑ_{sc} is 300^{0}C; ϑ_c is 105 ^{0}C.

After calculating this, time of thermal stability can be calculated by the next formula

$$t_{sc} = \frac{A_{th\_s}}{I_{br}{}^2}, \tag{2.8}$$

$$t_{sc} = \frac{9.1285 \cdot 10^6}{480^2} = 39.6203\ s.$$

Obtained value of thermal stability should not be less than 5 s.

2.2 Contact connections

The following view of dismountable contact connections was chosen:

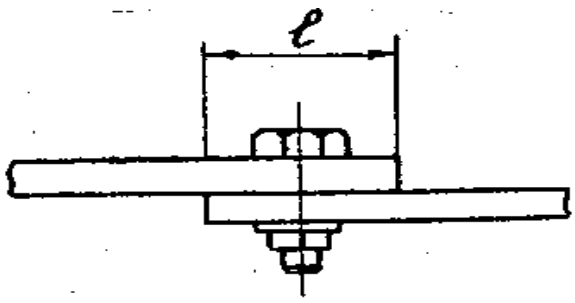

Figure 2.2 – The view of contact connections

The temperature of details in the contacting point can be determined by the formula

$$\vartheta_{\text{cont}} = \vartheta_{\text{set}} + \frac{{I_n}^2 \cdot R_{\text{cont}}}{k_t \cdot (S_{\text{c1}} - S_{\text{bolt}})}, \quad (2.9)$$

where R_{cont} – is a total resistance of the contact connection;

S_{c1} – is an area of a total external surface of the contact connection;

S_{bolt} – cross section of a chosen bolt.

Total resistance of the contact connection R_{ct} consists of transitional resistance of the contact R_c and of ohmic resistance R_{c1} of conductor parts, forming the contact connection

$$R_{cont} = R_c + R_{c1}\,. \quad (2.10)$$

Transitional resistance of the contact can be calculated by formula

$$R_c = \frac{\varepsilon_{sur}}{m_1 \cdot {P_k}^{m_2}}, \quad (2.11)$$

where ε is a factor, depending on the material and the state of the contact surface, Ohm·N; ε is $0.24 \cdot 10^{-2}$ Ohm·N;

m_1 is number of the bolts in the contact connection;

P_c is a force of contact pressure, N;

m_2 is a factor, depending on a number of contacting points and contact type (for two-dimensional contact m_2 is 0,7…1,0).

Force of contact pressure P_k is determined by recommended values of specific contact pressure p_k and by the area of contacting surface S_c

$$P_k = p_k \cdot S_{c.} \quad (2.12)$$

Specific pressure p_k in contacting parts, connected by bolts for copper is equal to 600 N/cm^2.

In the simplest case area of contacting surface S_c can be calculated by the next formula

$$S_c = \frac{I_n}{J_m}, \tag{2.13}$$

where j is equal to 0.31 A/mm^2 for copper buses with alternative current less than 200 A with frequency 50 Hz.

$$S_c = \frac{80}{0.31 \cdot 100} = 2.5806 \text{ cm}^2.$$

Substituting S_c to the formula (2.12), the force of contact pressure is next

$$P_k = 600 \cdot 2.5806 = 1548.3871 \text{ N}.$$

By value P_k from the table 22-3[18] 1 bolt M6 is chosen, m_1 is equal 1.

Inequality $P_{c\_bolt} > P_k$; 2.9 kN >1.5 kN is satisfied.

According to obtained contact pressure P_c transitional resistance of the contact R_c can be defined:

$$R_c = \frac{0.24 \cdot 10^{-2}}{1 \cdot 1548.3871^{0.85}} = 4.6646 \cdot 10^{-6} \text{ Ohm}.$$

Resistance R_{c1} differs from resistance of a straight line section of contacting parts because of current lines curvature at the contact point. It is taken into account by correction factor K_c, specified by the dependence $K_c = f\left(\frac{1}{a}\right)$ in [18].

Resistance R_{c1} of conductor parts, forming the contact connection can be calculated by formula

$$R_{c1} = k_c \cdot \frac{\rho_0 \cdot l}{k_t \cdot (S_c - S_{bolt})}, \quad (2.14)$$

where S_{bolt} is the cross-section of bolt, that is equal to $2 \cdot \pi \cdot d^2 / 4$;

l is a length of contact connection, cm; l is 2.726 cm;

ρ_0 is specific electrical resistance and it is equal to $1.62 \cdot 10^{-6}$ Ohm·cm;

$$S_{c1} = S_c - S_{bolt},$$

where S_c is the area of contacting surface, calculated by formula (2.4);

d is diameter of the M6 bolt in the corresponding table in [18], it's equal to 0.65 cm;

$$S_{c1} = 2.5806 - 2 \cdot 3.14 \cdot \frac{0.4225^2}{4} = 1.9173 \text{ cm}^2.$$

$$K_c = f\left(\frac{1.9173}{0.18}\right) = f(10.651) = 0.55.$$

After determining of all parameters, resistance R_{c1} of conductor parts can be defined as

$$R_{c1} = 0.55 \cdot \frac{1.62 \cdot 10^{-6} \cdot 2.726}{7 \cdot 10^{-4} \cdot 1.9173} = 1.2668 \cdot 10^{-6} \text{ Ohm}.$$

To calculate total resistance of the contact connection R_{cont} obtained transitional resistance of the contact R_c and ohmic resistance R_{c1} of conductor parts are substituted into the formula (2.10)

$$R_{\text{cont}} = 4.6646 \cdot 10^{-6} + 1.2668 \cdot 10^{-6} = 5.9314 \cdot 10^{-6} \text{ Ohm.}$$

The temperature of details in the contacting point now can be calculated by formula (2.9)

$$\vartheta_{\text{cont}} = 84.7891 + \frac{80^2 \cdot 5.9314 \cdot 10^{-6}}{7 \cdot 10^{-4} \cdot 1.9173} = 113.0734 ℃.$$

2.3 Switching contacts

The primary aim of the calculation is to establish the requisite contact pressure force, ensuring the contact point temperature stays within safe limits and preventing unwanted welding or spontaneous opening due to electrodynamic forces.

For enhanced contact durability, ceramic metal is recommended as the optimal material for contact plates. Although it may escalate initial costs, its use leads to improved arc stability, heightened reliability, and extended apparatus lifespan, outweighing the initial investment.

In constructing the AC contactor, silver with cermet has been selected for the contact plates. For bridge contacts, the width of the movable contact should either match or be slightly larger (up to 25%) than the current-carrying bus or flexible connection width.

Width of movable contact is

$$b_{\text{m\_c}} = 1.2 \cdot b, \tag{2.15}$$

$$b_{\text{m\_c}} = 1.2 \cdot 1 = 1.2 \text{ cm.}$$

The nearest standard value of movable contact width is chosen $b_{m.c}$ is 1.044 cm due to ГОСТ 3884-67.

Length of movable contact l is equal to 2 cm.

Perimeter of movable contact is

$$p_1 = 2 \cdot (l + b_{\text{m\_c}}), \tag{2.16}$$
$$p_1 = 2 \cdot (2 + 1.2) = 6.4 \text{ cm}.$$

Section of contact details by contact line is defined by formula

$$S_{\text{m\_c}} = l \cdot b_{\text{m\_c}}, \tag{2.17}$$
$$S_{\text{m\_c}} = 2 \cdot 1.2 = 2.4 \text{ cm}^2.$$

In the continuous mode of I_n current flow the transitional contact resistance with taking into account the influence of electric arc on contact heating is defined by the following expression [17]

$$S_{\text{m\_c}} = l \cdot b_{\text{m\_c}}, \tag{2.17}$$

$$\vartheta_m - \vartheta_{env} = \vartheta_{set} + \frac{R_{tr\_c} I^2 + P_{el.arc}}{2\sqrt{\lambda K_T p_1 S}_{m\_c}} + \frac{R_{tr\_c}^2 \cdot I_n^2}{8\lambda\rho_0(1+\alpha\vartheta_c)}, \tag{2.18}$$

where ϑ_m – is maximal temperature of contact surface, °C;

ϑ_c – is the temperature of contact detail that 84.7891 °C;

S_{m_c} – is section of contact details by contact line, cm^2; $S_{m\_c} = 2.4$ cm^2;

$P_{el.arc}$ – is the part of power losses from electric arc presence in apparatus contacts, W;

λ – is thermal conductivity factor of contact plates material; λ is 4.16 $\frac{\text{Wt}}{\text{cm} \cdot °\text{C}}$.

The part of power losses caused by electric arc in apparatus contacts is calculated by formula

$$P_{el.arc} = \frac{0{,}1 \cdot U_a \cdot I_a \cdot t_a \cdot Z}{3600}, \quad (2.19)$$

where U_a – is an arc voltage, V;

I_a – is an arc current, A;

t_a – is duration of arc burning on contacts, s.

For calculation of AC arc blow out device the duration of arc burning t_a is equal to 0.0015 s, and the arc voltage U_a is equal to 0.5-0.8 of U_n, U_a is 247 V.

The arc current is

$$I_a = \frac{I_n}{2}, \quad (2.20)$$

$$I_a = \frac{80}{2} = 40 \text{ A}.$$

Substituting obtained values into the formula (2.19) the part of power losses caused by electric arc in apparatus contacts can be calculated as:

$$P_{el.arc} = \frac{0.1 \cdot 247 \cdot 50 \cdot 0.0015 \cdot 1200}{3600} = 0.494$$

Contact pressure force is defined by expression

$$P_{c1} = \rho_{sp} \cdot I_n, \quad (2.21)$$

where ρ_{sp} – is a specific contact pressure on 1 A of rated current, N/A. For silver contacts of contactors it is equal to 0,07–0,145 N/A.

$$P_{c1} = 0.1 \cdot 80 = 8 \text{ N}.$$

The value of transitional contact resistance R_{tr_c} is calculated by formula

$$R_{tr.c} = \frac{K_1\left(1+\frac{2}{3}\alpha\vartheta_c\right)}{(0.102\cdot P_{c1})^m}\ , \qquad (2.22)$$

where K_1, m – are empirical coefficients; it's chosen from [17] in dependence on material and type of contacts, K_1 is 0.00006, m.

$$R_{tr\_c} = \frac{0.00006\cdot\left(1+\frac{2}{3}\cdot 0.0043\cdot 84.7891\right)}{(0.102\cdot 8)^1} = 0.0001\,\text{Ohm}.$$

Correctness of calculation of contact pressure force is checked by the temperature of contact surface. The value of ϑ_{cs} shouldn't exceed ϑ_m

$$\vartheta_{cs} = \vartheta_{set} + \frac{R_{tr\_c}I_n^2 + P_{el.arc}}{2\sqrt{\lambda K_T p_1}\cdot S_{m\_c}} + \frac{R_{tr\_c}^2\cdot I_n^2}{8\lambda\rho_0(1+\alpha\vartheta_c)}\ , \qquad (2.23)$$

$$\vartheta_{cs} = 84.7891 + \frac{0.0001\cdot 80^2 + 0.494}{2\sqrt{4.16\cdot 7.5\cdot 10^{-4}\cdot 6.088}\cdot 2.4} + \frac{0.0001^2\cdot 80^2}{8\cdot 4.16\cdot 1.59\cdot 10^{-6}\cdot(1+0.0043\cdot 84.7891)} =$$

$$= 89.797^{\circ}C.$$

In the short-term $t_{s.c.}$ regime of current $I_{s.c}$ flowing it should be determined whether the calculated contact pressure force P_{c1} will provide no welding of contacts.

Welding current is calculated by the following formula

$$I_w = \sqrt{\frac{\lambda\cdot P_{c1}\cdot(\vartheta_{melt}-\vartheta_{cs})}{0.1\cdot\rho\cdot\sigma_{sm}}\cdot\exp\left(\frac{C\cdot\gamma}{\lambda}\cdot\sqrt{\frac{P_{c1}}{3.14\cdot\sigma_{sm}\cdot t_{sc}}}\right)}, \qquad (2.24)$$

where ϑ_{melt} – is melting temperature of contact plates material, $^{\circ}C$; it is $961^{\circ}C$;

γ – is density of the contact plates material, g/cm^3; for silver with cadmium oxide γ is 10 g/cm^3;

ρ – specific electric resistance of the contact plates material; for silver with cadmium oxide $\rho = 1.59 \cdot 10^{-6}$ Ohm · cm ;

C – is specific heat of the contact plates material, J/g·deg; it is 0.234 J/g·deg;

σ_{com} – is ultimate compression strength of contact plates material, N/cm^2; for silver with cadmium oxide σ_{com} is 30300 N/cm^2.

$$I_w = \sqrt{\frac{4.16 \cdot 8 \cdot (961 - 89.797)}{0.1 \cdot 1.59 \cdot 10^{-6} \cdot 30300} \cdot \exp\left(\frac{0.234 \cdot 10}{4.16} \cdot \sqrt{\frac{8}{3.14 \cdot 30300 \cdot 5}}\right)} = 2.454 \cdot 10^3 A.$$

Contacts with calculated contact pressure force will not weld on, because the expression $I_{br} < I_w$ is satisfied.

For estimation of value of electrodynamics repulsion forces of contacts in case of short-circuit current flowing the following formula is used [17]

$$P_{el\_ef} = 2 \cdot 10^{-7} I_{br}^2 \ln \frac{S_{m\_c.}}{S_o}, \qquad (2.25)$$

where S_0 – is the section area of compression contact surface, that calculated by formula

$$S_o = \frac{\pi \cdot d_0^{\,2}}{4}, \qquad (2.26)$$

where d_0 – is a diameter of contact by contact line and it is defined by expression

$$d_o = 2 \cdot \sqrt{\frac{P_{c1}}{3.14 \cdot \sigma_{com}}}, \qquad (2.27)$$

$$d_o = 2 \cdot \sqrt{\frac{8}{3.14 \cdot 30300}} = 0.0183 cm.$$

Substituting the value of d_0 into formula (2.26) section area of compression contact surface is obtained

$$S_o = \frac{3.14 \cdot 0.0183^2}{4} = 0.0003 cm^2 .$$

Now the electrodynamics forces can be defined by formula (2.25)

$$P_{el\_ef} = 2 \cdot 10^{-7} 480^2 \cdot \ln \frac{2.4}{0.0003} = 0.42 \text{ N} .$$

In efficiently designed contact system the following condition should be execute

$$P_{el.ef} < P_{c1,}$$

$$0.42 \text{ N} < 8 \text{ N}.$$

Depending on alternative rated current of contactor the following contacts opening β is chosen

$$\beta = 5 \text{ mm}.$$

2.4 Calculation of wearing and follow through of contacts

Linear wearing of contacts can be determined by given number of circuit openings N_{el}, which apparatus contacts should stand. By linear contacts wearing the follow through of contacts, which should be 1,5-2,5 times greater than linear wearing, can be specified, i.e.

$$\sigma_f \approx (1{,}5 \ldots 2{,}5) \cdot \sigma_L \qquad (2.28)$$

The mass of the material, g, of one contacts pair, being used up, can be approximately calculated by formula

$$Q \approx 10^{-9} \cdot K_u \cdot N_{el} \cdot I_{br}{}^2, \qquad (2.29)$$

where K_u – is an empirical factor, depending on the current and contacts material, it is chosen by figure 1.3; K_u is 0.2 g/A^2.

Now by formula (2.29) the mass of material of one contacts pair can be calculated

$$Q = 10^{-9} \cdot 0.2 \cdot 10^6 \cdot 80^2 = 1.28\ g.$$

Volume wear can be defined by following expression

$$V = \frac{Q}{\gamma}, \qquad (2.30)$$

$$V = \frac{1.28}{10} = 0.128\ \text{cm}^3.$$

Knowing geometrical dimensions of the contact, the linear wearing can be found by volume wear V

$$\sigma_L = \frac{V}{S_{m\_c}}, \qquad (2.31)$$

$$\sigma_L = \frac{0.128}{2.4} = 0.0533\text{cm}.$$

And now by formula (2.28) the follow through of contacts can be assumed as

$$\sigma_f = 2 \cdot 0.0533 = 0.1067\ \text{cm}.$$

3 DESIGNING OF APPARATUS MECHANISM

Electromagnetic contactors function through the integration of two distinct mechanisms: an electromagnetic drive responsible for engaging the contactor and a spring mechanism tasked with disengagement. To properly calculate the electromagnetic mechanism performance, it is critical to first assess the characteristics of the opposing forces, which originate from the spring mechanism.

The spring mechanism consists of two primary components: the contact springs and the pullback springs. These springs create the necessary force to separate the armature from the core once the electromagnetic drive is de-energized. The contact springs exert pressure to maintain reliable electrical contact, while the pullback springs ensure the armature returns to its original position after operation.

To calculate the spring forces, the process requires specific initial parameters: for the contact springs: the preliminary compression force (P_1) and final compression force (P_2); for the pullback springs: the preliminary compression force (P_{1pb}) and final compression force (P_{2pb}).

These forces are critical in ensuring smooth contactor operation and preventing excessive wear or malfunction.

In order to calculate the values of P_1 and P_2 for the contact spring, the previously determined contact pressure force (P_c) must be adjusted. This adjustment involves realigning the force to the axis of the contact spring based on a design sketch that includes preliminary linear dimensions. This ensures the correct transmission of forces within the system and accounts for any deviations caused by spring placement or geometry.

The formula for adjusting the contact pressure to align with the contact spring's axis is next:

$$P_c' = 2 \cdot P_{c1}\ , \tag{3.1}$$

where P_{c1} - is contact pressure force, N; P_{c1} = 8 N;

$$P_c^{'} = 2 \cdot 8 = 16 \text{ N}.$$

The ratio between preliminary P_1 and final P_2 compression of contact spring can be assumed as

$$P_1 = 0.6 \cdot P_2 \tag{3.2}$$

The value of P_2 can be derived from expression

$$P_c^{'} = \frac{P_1 + P_2}{2} = \frac{0.6 \cdot P_2 + P_2}{2} = 0.8 \cdot P_2, \tag{3.3}$$

$$P_2 = \frac{P_c^{'}}{0.8}, \tag{3.4}$$

$$P_2 = \frac{16}{0.8} = 20 \text{ N}.$$

By the value of the final compression P_2 the value of preliminary compression P_1 can be determined as

$$P_1 = 0.6 \cdot 20 = 12 \text{ N}.$$

The value of initial force of pullback spring P_{1pb} is taken by the value of the final spring compression P_2, reduced to the axis of pullback spring. For apparatus with valve type electromagnet and normally open contacts

$$P_{1pb} = 0.3 \cdot \frac{3}{2} \cdot P_2, \tag{3.5}$$

K – is the number of the main apparatus contacts; K is 1.

$$P_{1pb} = 0.3 \cdot \frac{3}{2} \cdot 20 = 9 \text{ N}.$$

The final pressure of pullback spring P_{2pb} approximately can be assumed

$$P_{2pb} = 1.3 \cdot P_{1pb}, \tag{3.6}$$

$$P_{2pb} = 1.3 \cdot 9 = 11.7 \text{ N}.$$

The force of electromagnet which it can develop at critical air gap σ'_f is calculated by the following formula

$$P_{el\_cr.} = K_{saf} \cdot (P_{2pb} + 3 \cdot P_2), \tag{3.7}$$

where K_{saf} - safety factor, for contactors is equal to 1.3…1.7;

P_{cr} – the value of total opposing force at critical air gap;

$$P_{el.cr.} = 1.35 \cdot 71.7 = 96.795 \text{ N}.$$

Using the calculated values of the preliminary compression force (P_1) and final compression force (P_2) for the contact springs, along with the preliminary compression force (P_{1pb}) and final compression force (P_{2pb}) for the pullback springs, and the electromagnet force developed at the critical air gap (P_{el_cr}), there can be estimated the approximate characteristics of the opposing forces in the contactor.

These opposing forces represent the mechanical resistance the electromagnetic drive must overcome to actuate the contactor.

Since the pulling characteristic of an alternating current contactor is nearly linear, the critical electromagnet force (P_{el_cr}) is less significant to focus on. The most crucial point in this analysis is the upper limit on the opposing force characteristic P_{up}, which is determined from formula (3.7):

$$P_{up} = (P_{2pb} + 3 \cdot P_2), \quad (3.8)$$

$$P_{up} = 71.7 \text{ N}.$$

Drawn characteristics of opposing forces shown on figure 3.1.

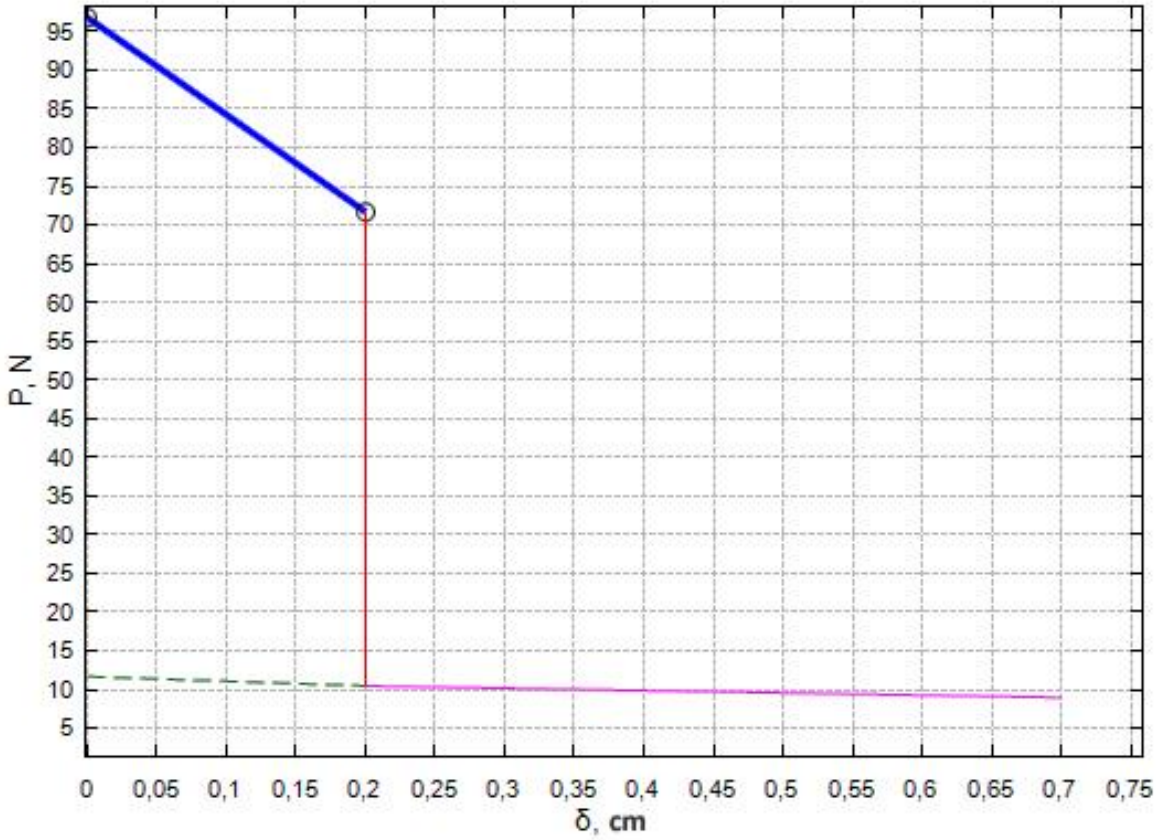

Figure 3.1 - Characteristic of opposing forces

4 PRELIMINARY CALCULATION OF ELECTROMAGNET

The aim of calculation is preliminary determination of magnetic circuit dimensions, magnetizing force of winding and its geometrical dimensions.

The magnetic starter has the electromagnet of alternative current of E-type.

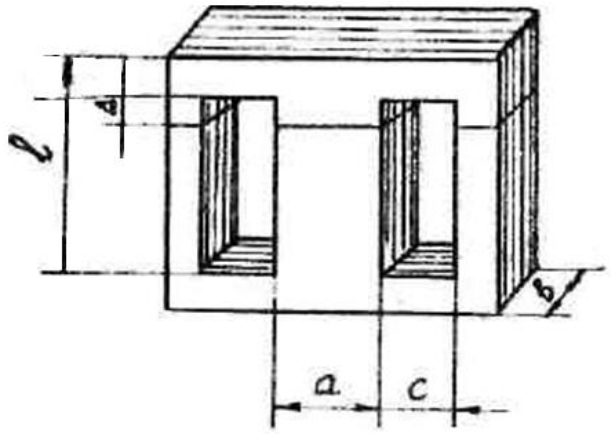

Figure 4.1 - Layer magnetic E-core

Cross-sectional area of the core is calculated by the following formula

$$S_c = \frac{P_{el\_cr}}{19.9 \cdot B_\delta^2}, \quad (4.1)$$

where P_{el_cr} is the force of electromagnet, which it can develop at critical air gap σ'_f ; $P_{el.cr.} = 1.35 \cdot 71.7 = 96.795$ N.

B_δ – magnetic induction in air gap, T; B_δ lies in the range 0,5 - 0,9 T.

$$S_c = \frac{96.795}{19.9 \cdot 0.8^2} = 7.6001 \text{ cm}^2.$$

Determination of core sides a and b:

$$\mathrm{a} = \frac{S_c}{K_{filling} \cdot b}, \tag{4.2}$$

where $K_{filling}$ is fill factor that is equal to 0.9 due to the width of the sheets 0.35mm.

Thus in layer magnetic core the perfect ratio is a/b=1

$$\mathrm{a} = \sqrt{\frac{S_c}{K_{filling}}}, \tag{4.3}$$

$$\mathrm{a} = \sqrt{\frac{7.6001}{0.9}} = 2.906 \text{ cm}.$$

The sectional area of the armature is determined by

The width of basic size

$$l_{basic} = \sqrt{S_c} = \sqrt{\mathrm{a} \cdot \mathrm{b}}, \tag{4.4}$$

$$\mathrm{l_{basic}} = \sqrt{7.6001} = 2.7568 \text{ cm}.$$

The width of the opening

$$C = C^* \cdot \mathrm{a}, \tag{4.5}$$

where $C^* = 0.8 \ldots 1.2$;

$$\mathrm{C} = 0.8 \cdot 2.906 \ = 2.3248 \text{ cm}.$$

The average length of wind

$$\mathrm{l_{average}} = 2 \cdot (\mathrm{a} + \mathrm{b}) + 4 \cdot \mathrm{C}, \tag{4.6}$$

$$\mathrm{l_{average}} = 2 \cdot (2.906 + 2.906) + 4 \cdot 2.3248 = 20.9229 \text{ cm}.$$

The opening height

$$l_h = \frac{0.33 \cdot l_{average} \cdot \sqrt{l_{basic}}}{c}, \tag{4.7}$$

$$\mathrm{l}_h = \frac{0.33 \cdot 20.9229 \cdot \sqrt{2.7568}}{2.3248} = 4.9313 \text{ cm}.$$

The number of turns

$$W = \frac{K_{n\_min} \cdot U_n \cdot K_r}{4.44 \cdot f \cdot B_{\delta max\_out} \cdot S_c}, \tag{4.8}$$

where $K_{\mathrm{n\_min}}$ is 0.7 is the coefficient that takes minimal possible voltage of network into account;

$B_{\delta \mathrm{max\_out}}$ - is equal to 1 T;

$\mathrm{K_r}$ - is the coefficient that takes into account the voltage drop in active resistance and it equals to 0.9;

$$\mathrm{W} = \frac{0.7 \cdot 380 \cdot 0.9}{4.44 \cdot 50 \cdot 0.9 \cdot 7.6001 \cdot 10^{-4}} = 1419.$$

The cross-sectional area of wire

$$g_m = \frac{S_c}{W}, \tag{4.9}$$

where $\mathrm{K_{зм}}$ is fill factor of the coil, it's equal to 0.2…0.22.

$$\mathrm{g_m} = \frac{7.6001}{1419} = 0.0048 \text{ cm}^2.$$

Magnetizing force of winding operation is calculated by

$$\mathrm{F}_{av} = \frac{B_{\delta \max\_out}}{\mu_0 \cdot \sigma_{\text{bulging}}} \cdot \delta_{\text{sum\_attr\_eq}}, \quad (4.10)$$

where $\delta_{\text{sum\_attr\_eq}}$ - is equivalent summary gap, which is equal to 0.002 m.

σ_{bulging} is equal to 1…1.8.

$$\mathrm{F}_{av} = \frac{1}{1.256 \cdot 10^{-6} \cdot 1} \cdot 0.002 = 1592 \text{ A}.$$

The maximal coil current, not taking into account inductive resistance of winding

$$R = \frac{\rho_0 \cdot (1 + \alpha_c \cdot \vartheta_c) \cdot l_{average}}{g_m} \cdot W, \quad (4.11)$$

$$\mathrm{R} = \frac{1.62 \cdot 10^{-6} \cdot (1 + 0.0043 \cdot 105) \cdot 20.9229}{0.0048} \cdot 1419 = 14.4808 \text{ Ohm},$$

The value of current in closed state of armature

$$I = \frac{1.05 \cdot U_n}{\sqrt{R^2 + X^2}}, \quad (4.12)$$

where X is inductive resistance

$$\mathrm{X} = \omega \cdot \mathrm{L}, \quad (4.13)$$

$$\mathrm{L} = \mathrm{W}^2 \cdot Л_\delta, \quad (4.14)$$

$$Л_\delta = \mu_0 \cdot \frac{\mathrm{S_c}}{\delta_{\text{sum\_attr\_eq}}}, \quad (4.15)$$

$$Л_{\delta} = 1.256 \cdot 10^{-6} \cdot \frac{7.6001 \cdot 10^{-4}}{0.002} = 4.7729 \cdot 10^{-7},$$

$$\mathrm{L} = 1419^2 \cdot 4.7729 \cdot 10^{-7} = 0.9609 \text{ H},$$

$$\mathrm{X} = 2 \cdot 3.14 \cdot 50 \cdot 0.9609 \ = 301.7253,$$

$$\mathrm{I} = \frac{1.05 \cdot 380}{\sqrt{301.7253^2 + 14.4808^{\,2}}} = 1.3209 \text{ A}.$$

Magnetizing force of electromagnet at a moment of operation

$$\mathrm{F} = \mathrm{I} \cdot \mathrm{W}, \tag{4.16}$$

$$\mathrm{F} = 1.3209 \ \cdot 1419 = 1874 \text{ A}.$$

As $\mathrm{F} \geq \mathrm{F_{av}}$ is satisfied, the calculations can be considered as suitable.

$$1874 \text{ A} \geq 1592 \text{ A}.$$

Steady-state temperature-rise is calculated due to Newton's formula

$$\tau_{\mathrm{set}} = \frac{\sum \mathrm{P}}{\mathrm{k_{TO}} \cdot \mathrm{S}_{cooling}}, \tag{4.17}$$

where $\mathrm{k_{TO}}$ is the heat transfer coefficient that is determined by the dependence between the coefficient and temperature-rise $\mathrm{K_T}$ in steel; it is equal to $67 \ \mathrm{W/m \cdot C}$;

$\sum \mathrm{P}$=$P_{\mathrm{steel}} + P_{\mathrm{eddy\_cur}} + P_{\mathrm{act\_wind}}$ is the summary losses.

Now the losses are needed to be calculated.

The losses in steel:

$$P_{\text{steel}} = k_{\text{g}} \cdot P_{\text{r\_b}} \cdot G_{\text{st}}, \quad (4.18)$$

where k_{g} is experimental coefficient, which is equal 2-3;

$P_{\text{r\_b}}$ is specific loss for B_{m}= 1.5T that is determined from the dependence of the graph in [18] and it's equal to 2.1 VA/kg.

G_{st} is the mass of steel

$$G_{\text{st}} = \rho_0 \cdot V_{\text{st}}, \quad (4.19)$$

where ρ_0 for steel is equal to 7.65· 10^3kg/m^3;

$$G_{\text{st}} = 7.65 \cdot 10^3 \cdot 41897.65 = 0.3205 \text{ kg},$$

$$P_{\text{steel}} = 2 \cdot 2.1 \cdot 0.3205 = 1.3462 \text{ W}.$$

Magnetic losses

$$P_{\text{act\_wind}} = I^2 \cdot R, \quad (4.20)$$

$$P_{\text{act\_wind}} = 1.3209^2 \cdot 14.4808 = 25.265 \text{ W}.$$

The summery losses

$$\sum P = P_{\text{steel}} + P_{eddy\_cur} + P_{act\_wind} = (2.4 \dots 2.5) \cdot \left(P_{\text{steel}} + P_{act\_wind}\right), \quad (4.21)$$

For calculating $S_{cooling}$ should be found. It can be calculated by next formula

$$S_{cooling} = a \cdot b \cdot l_{average} - 2 \cdot ((a - 2 \cdot l_h) \cdot (b - 2 \cdot C)), \quad (4.22)$$

$$S_{cooling} = 2.906 \cdot 2.906 \cdot 20.9229 - 2 \cdot ((2.906 - 2 \cdot 4.9313) \cdot (2.906 - 2 \cdot 2.3248)) = 152.4257\ cm^2.$$

$$\tau_{set} = \frac{2.4 \cdot (25.265 + 1.3462)}{67 \cdot 152.4257 \cdot 10^{-4}} = 62.5378\ ^0\text{C}.$$

It compares with permissible temperature for A class insulation.

$$\tau_{set} + \vartheta_{env} < \vartheta_c,$$

$$102.5378\ ^0\text{C} < 105\ ^0\text{C}.$$

The preliminary calculations are finished. The dimensions have been chosen correctly.

5 CALCULATION OF ARC CONTROL SYSTEM

The arc blowout method using a double loop break is particularly effective for breaking circuits with voltages ranging from 220V to 380V and frequencies between 50Hz and 500Hz. This technique is employed to interrupt the current and extinguish the arc formed when opening high-power circuits. By fulfilling these voltage and frequency specifications, this method ensures reliable performance in such conditions, making it suitable for a wide range of industrial applications.

The recovery voltage of contacting gap

$$U_{\text{от}} = \frac{1.1 \cdot \sqrt{2} \cdot \text{U}_\text{n}}{\sqrt{3}} \cdot \text{k}_{\text{сх}} \cdot \sin(\varphi), \quad (5.1)$$

where $\text{k}_{\text{сх}}$ is 1.5 – the scheme coefficient;

φ is the angle of phase displacement and it is equal to 66.5 ^{0}C.

$$U_{\text{от}} = \frac{1.1 \cdot \sqrt{2} \cdot 380}{\sqrt{3}} \cdot 1.5 \cdot \sin(1.161) = 469.5555 \text{ V}.$$

where f_0– is fundamental frequency, which is equal 5 000…20 000 Hz [18];

k_a is am amplitude coefficient

$$\text{k}_\text{a} = \frac{U_{\text{v\_max}}}{U_{\text{от}}} \approx 1 + \text{e}^{-0.0003 \cdot \text{f}_0}, \quad (5.2)$$

$$\text{k}_\text{a} = 1 + \text{e}^{-0.0003 \cdot 7000} = 1.1225.$$

The inductance of interrupted circuit

$$\text{L} = \frac{\text{U}_\text{n} \cdot \sin \varphi_0}{I_{\text{br}} \cdot \omega}, \quad (5.3)$$

$$L = \frac{380 \cdot \sin(1.161)}{480 \cdot 2 \cdot 3.14 \cdot 50} = 0.0023 \text{ H.}$$

The length of the arc can be calculated by next formula

$$l_{d0} = \sqrt{\delta_k + 12300 \cdot I_{br}^{\frac{2}{3}} \cdot 0.01^2}, \quad (5.4)$$

where δ_k is equal to 2,

$$l_{d0} = 8.798 \text{ cm.}$$

Active resistance of the arc

$$R_д^0 \approx 0.015 + \frac{14200}{I_{br}^2}, \quad (5.5)$$

$$R_д^0 \approx 0.015 + \frac{14200}{480^2} = 0.0766 \text{ Ohm.}$$

The equivalent resistance of arc on one pole

$$R_д \approx R_д^0 \cdot n \cdot l_{d0}, \quad (5.6)$$

where n is the number of breaks on one pole; n=1.

$$R_д \approx 0.0766 \cdot 1 \cdot 8.798 = 0.6742 \text{ Ohm.}$$

Now the number of breaks needs to be recalculated to check if it is enough to blow the arc out

$$n_{a\_cal} = \frac{k_n \cdot U_n - A_x\left(1 + \ln\frac{k_n \cdot U_n}{A_x}\right)}{U_{v.p.}^0 + 0.34 \cdot k_n \cdot l_{d0} \cdot R_d^0 \cdot I_{br}}, \quad (5.7)$$

where k_n, A_x and M_0 are the coefficients, which are

$$k_n = 0.9 \cdot k_{cx} \cdot \sqrt{1 - \cos(\varphi)}, \quad (5.8)$$

$$k_n = 0.9 \cdot 1.5 \cdot \sqrt{1 - 0.4} = 1.046,$$

$$M_0 \approx 0.8 \cdot 10^{-5} + \frac{2.5}{I_{br}^2}, \quad (5.9)$$

$$M_0 \approx 0.8 \cdot 10^{-5} + \frac{2.5}{480^2} = 1.8851 \cdot 10^{-5},$$

$$A_x = \frac{k_\Sigma \cdot \beta_к \cdot L}{M_0}, \quad (5.10)$$

where $\beta_к = 2$ from the table [18];

k_Σ is 1.

$$A_x = \frac{1 \cdot 2 \cdot 0.0023}{1.8851 \cdot 10^{-5}} = 245.3468,$$

$$n_{a\_cal} = \frac{1.046 \cdot 380 - 245.3468(1 + \ln\frac{1.046 \cdot 380}{245.3468})}{70 + 0.34 \cdot 1.406 \cdot 8.798 \cdot 0.6742 \cdot 480} = 0.1831,$$

$$n_a > n_{a\_cal},$$

$$1 > 0.1831,$$

$$f_{0\_cal} = \frac{M_0 \cdot n_a \cdot 10^6}{\pi \cdot L}, \quad (5.11)$$

$$f_{0\_cal} = \frac{1.8851 \cdot 10^{-5} \cdot 1 \cdot 10^6}{3.14 \cdot 0.0023} = 2596 \text{ Hz},$$

$$2596 \text{ Hz} < 7000 \text{ Hz}.$$

Since all conditions are met, a single break is sufficient to effectively extinguish the arc. This eliminates the need for additional components such as arc chutes, shells, frames, or clenches. The single break design ensures simplicity in construction while maintaining reliable performance.

By avoiding the complexity of extra devices, this method not only reduces the overall cost but also improves the ease of maintenance and reliability of the system. The simplicity of the design, combined with the adequate arc suppression capability, makes it a highly efficient solution for circuit interruption within the specified voltage and frequency ranges.

6 THE CALCULATION OF SPRINGS

Springs play a critical role in many electrical devices, where they greatly impact performance and reliability. Among the various types, the cylindrical screw spring is particularly notable for its unique properties and adaptability. Its design allows for high resistance to bending forces, making it an ideal choice for numerous applications. The durability of cylindrical screw springs ensures long-lasting operation, especially in environments with frequent mechanical stress.

These springs are versatile, fitting into different apparatus configurations, whether in compact systems or large-scale industrial equipment. Their ability to efficiently store and release energy makes them indispensable in mechanical and electrical systems, where precise force application is required, such as in contactor mechanisms, switches, and other dynamic components.

All calculations are carried on by methods, stated in [18].

6.1 The calculation of contact spring

The initial data for the calculation:

- P_p is initial force of pullback spring which is equal to 9 N;
- f is bending which is equal to 2.2 mm;
- G is shift modulus which is equal to 80 000 N/mm^2;
- $\sigma_{p.st}$ is permissible torsional stress which is equal $580\ \mathrm{N/mm^2}$;
- c_n is spring index which is equal from 4 to 10 for the small diameters of the spring wire.

The diameter of spring wire

$$d = \sqrt{\frac{8 \cdot P_p \cdot c_n}{\pi \cdot \sigma_{p.st}}}, \tag{6.1}$$

$$d = \sqrt{\frac{8 \cdot 9 \cdot 6}{\pi \cdot 580}} \approx 0.487 \text{ mm.}$$

Spring diameter

$$D = d \cdot c_n, \tag{6.2}$$

$$D = 0.487 \cdot 6 = 2.9222 \text{ mm.}$$

Number of turns in spring

$$N = \frac{G \cdot d^4 \cdot 2 \cdot f}{8 \cdot D^3 \cdot P_p}, \tag{6.3}$$

$$N = \frac{80000 \cdot 0.487^4 \cdot 2 \cdot 2.2}{8 \cdot 9 \cdot 2.9222^3} = 11.0235 \text{ turns.}$$

The number of turns is taken as 12.

The actual bending of the spring

$$f_a = \frac{8 \cdot D^3 \cdot P_p \cdot N}{G \cdot d^4}, \tag{6.4}$$

$$f_a = \frac{8 \cdot 2.9222^3 \cdot 9 \cdot 12}{80000 \cdot 0.487^4} = 4.3906 \text{ mm.}$$

Checking of mechanical stress in the spring

$$\sigma = \frac{16 \cdot P_p \cdot D}{2 \cdot \pi \cdot d^3}, \quad (6.5)$$

$$\sigma = \frac{16 \cdot 9 \cdot 2.9222}{2 \cdot 3.14 \cdot 0.487^3} = 580 \ \frac{N}{mm^2},$$

$$\sigma \approx \sigma_{p.st},$$

$$580 \frac{N}{mm^2} = 580 \ \frac{N}{mm^2}.$$

6.2 The calculation of opposing spring

The initial data for the calculation:

- P_p is final force of pullback spring which is equal to 11.7 N;
- f is bending which is equal to 5 mm;
- G is shift modulus which is equal to 80 000 N/mm^2;
- $\sigma_{p.st}$ is permissible torsional stress which is equal $580 \ N/mm^2$;
- c_n is spring index which is equal from 4 to 10 for the small diameters of the spring wire.

The diameter of spring wire

$$d = \sqrt{\frac{8 \cdot P_p \cdot c_n}{\pi \cdot \sigma_{p.st}}},$$

$$d = \sqrt{\frac{8 \cdot 11.7 \cdot 6}{\pi \cdot 580}} \approx 0.5553 \text{ mm}.$$

Spring diameter

$$D = d \cdot c_n,$$

$$D = 0.5553 \cdot 6 = 3.3319 \text{ mm}.$$

Number of turns in spring

$$N = \frac{G \cdot d^4 \cdot 2 \cdot f}{8 \cdot D^3 \cdot P_p},$$

$$N = \frac{80000 \cdot 0.5553^4 \cdot 2 \cdot 5}{8 \cdot 11.7 \cdot 3.3319^3} = 21.9733 \text{ turns}.$$

The number of turns is taken as 22.

The actual bending of the spring

$$f_a = \frac{8 \cdot D^3 \cdot P_p \cdot N}{G \cdot d^4}, \quad (6.4)$$

$$f_a = \frac{8 \cdot 3.3319^3 \cdot 11.7 \cdot 22}{80000 \cdot 0.5553^4} = 9.5571 \text{ mm}.$$

Checking of mechanical stress in the spring

$$\sigma = \frac{16 P_p \cdot D}{2\pi \cdot d^3}, \quad (6.5)$$

$$\sigma = \frac{16 \cdot 11.7 \cdot 3.3319}{2 \cdot 3.14 \cdot 0.5553^3} = 580 \ \frac{N}{mm^2},$$

$$\sigma \approx \sigma_{p.st},$$

$$580 \frac{N}{mm^2} = 580 \ \frac{N}{mm^2}.$$

As the calculations are correct, the type of spring and its material is suitable for using in AC contactor of ПМ series.

The characteristics of chosen springs:

- material is carbon steel spring wire, ГОСТ 9389-60 for cold winding, high-strength material;
- material mark is I (B);
- ultimate strength during the tension is 2 650 N/mm^2;
- permissible torsional stress is 580 N/mm^2;
- permissible bending stress is 930 N/mm^2;
- shift modulus is 80 000 N/mm^2;
- strength modulus is 200 000 N/mm^2;
- electrical resistivity is 0.19-0.22 $\cdot$ 10^{-6} Ohm$\cdot$ m.

7 **MODELING IN THE FEMM PROGRAM**

7.1 Description of the FEMM program

The Finite Element Method Magnetics (FEMM) is an indispensable tool in electrical engineering and research for solving low-frequency electromagnetic problems in 2D and axisymmetric configurations. By utilizing FEMM, engineers can simulate complex electromagnetic fields, providing critical insights into how devices will perform under real-world conditions. The finite element method (FEM) used by the software allows precise calculations by dividing the electromagnetic fields into smaller elements, providing high accuracy in solving differential equations related to magnetic fields. This makes FEMM both powerful and user-friendly, allowing professionals to conduct in-depth studies on various electrical components.

Why analyze AC electromagnets in FEMM? Alternating current (AC) electromagnets are crucial in electrical devices such as transformers, electric motors, and inductors. These components rely on the alternating nature of current to generate varying magnetic fields, which in turn affect performance parameters like inductance, torque, and efficiency. By studying AC electromagnets in FEMM, researchers can:

- optimize design: ensuring the electromagnet is optimized for efficiency means minimizing energy losses and improving the performance of the device.
- predict performance: engineers can predict how the electromagnet will behave under varying loads and conditions, understanding how the magnetic fields fluctuate.
- minimize losses: FEMM helps identify energy losses due to eddy currents and hysteresis, allowing engineers to adjust the design for lower heat generation and higher energy efficiency.

- ensure safety: safety is paramount when dealing with high-power devices. FEMM enables the evaluation of thermal limits and mechanical stresses, ensuring the electromagnet operates within safe parameters.

Modeling AC electromagnets in FEMM.

1. Geometry creation: the first step involves drawing the shape and dimensions of the electromagnet, including the core, windings, and housing, using FEMM's graphical interface. This graphical interface makes it easy for engineers to accurately model the physical structure of the device.

2. Material properties: FEMM provides a library of materials with defined properties, such as conductivity and permeability. Materials like copper for windings and iron for cores can be selected from this library, or custom materials can be defined for more specific applications. Accurate material definition is essential for precise simulation results.

3. Boundary conditions: setting up boundary conditions ensures that the simulation reflects real-world working conditions. This includes inputting the AC voltage, current frequency, and external magnetic fields that the device will experience in operation. This step ensures that the simulation replicates the actual working environment of the electromagnet.

4. Mesh generation: once the geometry and conditions are set, the program divides the model into small elements (mesh). Mesh generation is crucial for accurate simulation. A finer mesh results in more accurate results but requires more computing power, whereas a coarser mesh might yield faster but less precise results.

Calculation of the critical parameters**.** After setting up the model, FEMM uses its solvers to do the calculations. For AC electromagnets, it solves the time-harmonic magnetic field equations. Important results include:

Magnetic field distribution: the program visualizes the magnetic flux density (B-field) and magnetic field strength (H-field) throughout the electromagnet, showing engineers where the field is strongest or weakest.

Inductance and impedance: these are critical parameters that describe how efficiently the electromagnet stores energy and how it resists AC current flow. These factors directly affect the performance and energy consumption of the device.

Eddy current losses: the program calculates where eddy currents are generated in conductive materials, highlighting areas where energy loss occurs as heat. This information helps engineers design for minimal energy wastage.

Force and torque: FEMM calculates the magnetic forces and torques exerted by the electromagnet, which are crucial for determining how the electromagnet interacts with other mechanical parts.

Outputting the final picture of magnetic fields. When the calculations are done, FEMM offers several ways to see the results:

Field plots: colorful pictures showing the magnetic field distribution. These pictures show the size and direction of the fields, making it easy to see areas with high flux density. Red might show strong fields, while blue shows weak fields.

Vector plots: images that show the direction and size of the magnetic fields at different points in the model. Arrows can show which way the field points and how strong it is.

Contour plots: lines that show areas of constant magnetic potential or flux density, useful for detailed study. These lines help understand how the field changes in space.

Data export: engineers can export data into formats such as spreadsheets for further analysis, or use it in other software tools. This flexibility allows for deeper examination and integration into larger engineering projects. FEMM supports exporting to different formats, like spreadsheets (Excel) and text files (TXT).

Reports: detailed reports summarizing the analysis results, including important numbers, pictures, and calculation data. This can be printed or saved for future use.

Using FEMM to study AC electromagnets helps engineers and researchers understand the electromagnetic behavior of their designs, improving performance,

efficiency, and safety. This means they can make better, safer, and more efficient electromagnets.

Taking a closer look at the program. The FEMM software package consists of four parts:

1. Dialog shell (femm.exe)

The dialog shell, or femm.exe, acts as the primary interface for users. It is a pre-processor program that provides a CAD-like environment for creating and defining the problem geometry. This component allows users to:

- Draw geometry: users can create the physical layout of the electromagnetic problem using intuitive drawing tools. The interface supports creating complex geometries with ease.
- Set material properties: users can specify the material characteristics of different areas within the model, including conductivity, permeability, and other essential parameters.
- Define boundary conditions: users can set up various boundary conditions that mimic real-world scenarios, essential for accurate simulations.
- Import CAD files: the program allows importing AutoCAD (.DXF) files, which can streamline the geometry creation process by enabling users to use pre-existing designs.

2. Triangulation program (triangle.exe).

The triangulation program, known as triangle.exe, is crucial for preparing the geometric model for simulation. This component performs the following functions:

- Mesh generation: it divides the solution area into triangular elements, which are essential for applying the finite element method. This division can be specified by the user or set to default parameters.
- Mesh quality control: users can ensure that the mesh quality meets the required standards for accurate simulation, which is critical for the precision of the results.

3. Solvers. FEMM includes several solvers that address different types of problems within electromagnetic analysis:

- fkern.exe: this solver is used for solving magnetic field problems, allowing users to analyze how magnetic fields distribute within the modeled geometry.
- belasolv.exe: this solver focuses on electrostatic problems, enabling the study of electric fields and potential distributions.
- hsolv.exe: designed for thermal problems, this solver allows users to analyze heat distribution and temperature effects within the model.
- csolv.exe: this solver addresses current distribution problems in conductors, helping users understand how current flows and where potential issues may arise.

Each solver generates a set of output files that describe the problem setup and provide detailed solutions, which can be used for further analysis and interpretation.

4. Dialog shell (femmplol.exe)

The final processor, or femmplol.exe, serves as the concluding component of the FEMM package. This program provides the following capabilities:

- Visualization of solutions: users can visualize the solutions to field problems in various formats, such as equipotential lines and flow lines, which depict how fields behave in the modeled area.
- Color mapping: the results can be represented as images, where color gradients correspond to specific values of calculated quantities (such as magnetic flux density or temperature). This visual representation aids in the quick identification of areas of interest or concern within the model.

Limitations in the use of the program.

The FEMM package is a powerful tool for solving a variety of electromagnetic problems; however, it has certain limitations that users must be aware of. Notably, the FEMM system does not solve Maxwell's equations in all scenarios. It is primarily designed to address magnetism problems that can be classified as "low-frequency problems". This classification means that it operates under the assumption that displacement currents are negligible compared to conduction currents.

In practical terms, this limitation implies that FEMM is not suitable for applications involving high-frequency phenomena, such as radio wave propagation,

where displacement currents play a significant role. As a result, users seeking to model scenarios involving such high-frequency behaviors may need to consider alternative software solutions capable of addressing the full spectrum of Maxwell's equations.

Furthermore, FEMM is primarily focused on two-dimensional (2D) analysis. This constraint may a little limit its applicability for complex geometries or systems that require a 3D representation for accurate results. Users should keep these limitations in mind when planning their projects, as they may need to supplement FEMM with additional computational tools or methodologies to fully capture the electromagnetic behavior of their designs in high-frequency or three-dimensional contexts.

7.2 Building a model of an AC electromagnet

To create a model, there are some important information and steps to consider first.

The preprocessor in FEMM serves as a critical tool for establishing the design geometry required for electromagnetic analysis. This process involves defining the materials of the geometry and setting appropriate boundary conditions to accurately simulate the physical scenario.

To create a new file in the FEMM environment, users initiate the process by selecting the «File» menu and then choosing «New». This action opens a dialog box, prompting the user to select the type of problem they intend to address. In this case, users should select «Magnetics Problem» to set up the environment specifically for magnetic field analysis.

Once the magnetic problem is selected, one can proceed to utilize the CAD-like interface to draw the desired geometry. The preprocessor allows for precise control over the dimensions and shapes, ensuring that the model accurately reflects the intended design. Users can also specify the material properties for different areas

of the geometry, allowing for a comprehensive understanding of how various materials will interact within the magnetic field.

Additionally, boundary conditions are crucial in defining how the system behaves at its edges or interfaces. These conditions can include specifications for the magnetic field or constraints on how the field lines are allowed to interact with the geometry. By carefully setting these parameters, users ensure that the simulation results are reliable and reflective of real-world behavior.

The drawing of design geometry in FEMM consists of four essential types of elements that contribute to the accurate representation of the physical problem being analyzed:

- Starting and ending points: these are the foundational points that define linear and arc segments within the geometry. The starting point marks the beginning of a segment, while the ending point indicates where it concludes. These points are crucial for establishing the shape and layout of the design.
- Connecting lines: This element includes both straight and arc segments that connect the starting and ending points, forming the structure of the geometry. The ability to create curves and angles allows for more complex shapes that closely resemble real-world applications.
- Block label markers: these markers are added to the geometry to define material properties and specify cell sizes for the computational grid. By assigning block labels, users can indicate which materials will occupy different areas of the geometry, facilitating accurate simulations that take into account the varying properties of different materials. The cell size affects the mesh density, which is essential for determining the precision of the finite element analysis.
- Boundary conditions: at the outer boundaries of the geometry, boundary conditions must be established. These conditions dictate how the electromagnetic fields interact with the edges of the modeled area. Properly defining boundary conditions is crucial for obtaining valid simulation results,

as they can significantly influence the behavior of the magnetic fields and the overall system response.

The key elements of using a preprocessor in FEMM are crucial for efficiently creating design geometries:

- spot mode: defines specific points in the geometry by clicking on desired locations, facilitating accurate placement.

- segment mode: allows users to draw linear segments by connecting points or dragging the mouse, forming the basic structure of the design.

- arc segment: enables the creation of curved lines or arcs, useful for representing circular or rounded features.

- block method: defines areas with the same material properties or mesh size, streamlining the modeling process.

- group method: organizes and manages different elements by grouping them, simplifying modifications and analyses.

There is also a grid and buttons for working with it: show/hide, snap a point to the grid, grid size.

Command sequence for drawing objects:

1. Switch to point drawing mode.
2. Specify point coordinates by left-clicking with grid snapping enabled or by pressing the Tab key to enter Cartesian or cylindrical coordinates in the dialog box.
3. For straight lines, switch to "Line Drawing" mode and left-click the corresponding points.
4. To draw segments, switch to "Segment Drawing" mode and left-click the corresponding points. In the dialog box, specify the arc angle, maximum discretization angle, and any necessary boundary conditions. The arc's convexity direction depends on the order of the specified points (positive direction of contour traversal).

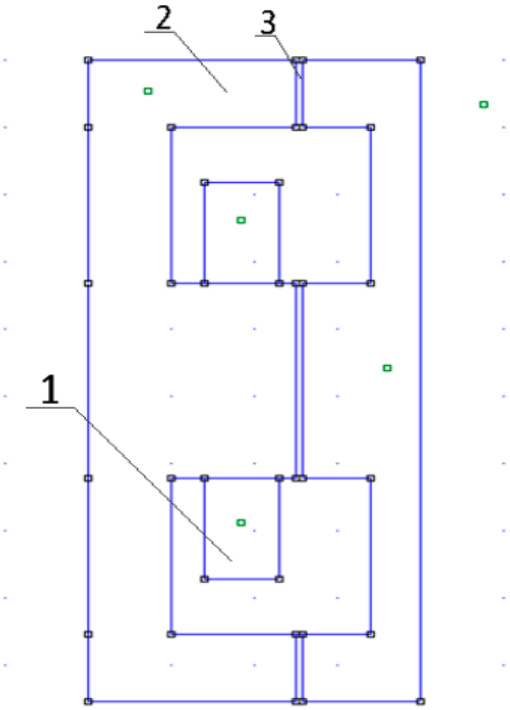

1 – coil; 2 – body of electromagnet; 3 – air gap.

Figure 7.1 – Built electromagnet of needed contactor:

6.3 Creating a model of an AC electromagnet, parameter output

After building the electromagnet, next, the user can either create a custom material or choose from a library of predefined materials. These actions are done through the "Properties of Materials" block, where material properties are assigned to the block label. To adjust properties, go to (Menu/Properties/Material). Modifications to existing materials are made using the (Modification) button, while new materials can be added with the (Add) button. Notably, materials from the library must be dragged into the appropriate column of the model with the mouse.

To create a custom material in FEMM, users can follow several key steps to define the material's properties accurately. Inside the dialog box, users can define various material characteristics that are essential for the accuracy of the simulation.

The process here is divided on several parts.

Magnetic properties:

- Relative permeability (μ_r), it defines the material's ability to conduct magnetic fields relative to free space. This value is crucial for modeling ferromagnetic materials like iron or steel.
- Coercivity (H_c): for permanent magnets, input the coercive force, which determines how strongly the material can retain its magnetization.

Electrical properties:

- Electrical conductivity (σ): it represents how easily the material allows electric current to flow. Materials like copper or aluminum will have high conductivity, while insulating materials will have low or zero conductivity.
- Laminate properties (for cores): there can be defined the type of core lamination, which is essential to reduce eddy currents in applications like transformers.

Thermal Properties (optional). For thermal simulations, it may be necessary to define the material's thermal conductivity and specific heat. This is useful for applications where heat dissipation is a factor, such as in motors or transformers.

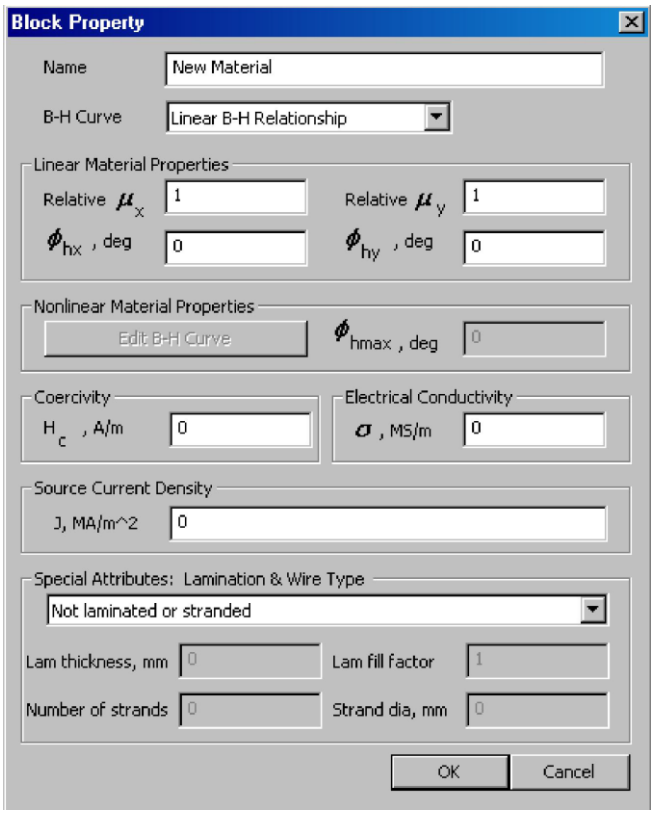

Figure 7.2 – View of creating material block

Once the new material is created or existing one dragged, it assigns to specific regions of the geometry. To do this, there need to use the block label tool and drag the new material from the library into the corresponding sections of the model.

Next step is to define the form of current in circuit, is it series or parallel connection of elements and value of current.

Selecting the "Series" option in FEMM indicates that one current flows through all the turns of the coil. In the "Properties of the selected block" dialog box, user must input the total number of series turns.

On the other hand, selecting the "Parallel" option assumes that there is only one turn with a total current flowing through it. In this case, the user must input the complex value of the current, which is expressed as Re(value) + I*Im(value), representing both the real and imaginary components of the current.

After writing in circuit series connection and setting 80A as a value of current, start to choose materials.

Then start with selecting the air for the external environment, after that select the steel material, 416 stainless steel. Next, select the wire for needed model, we put 10 AWG from the proposed ones, with a maximum permissible current of 140 amperes and set winds in our coil.

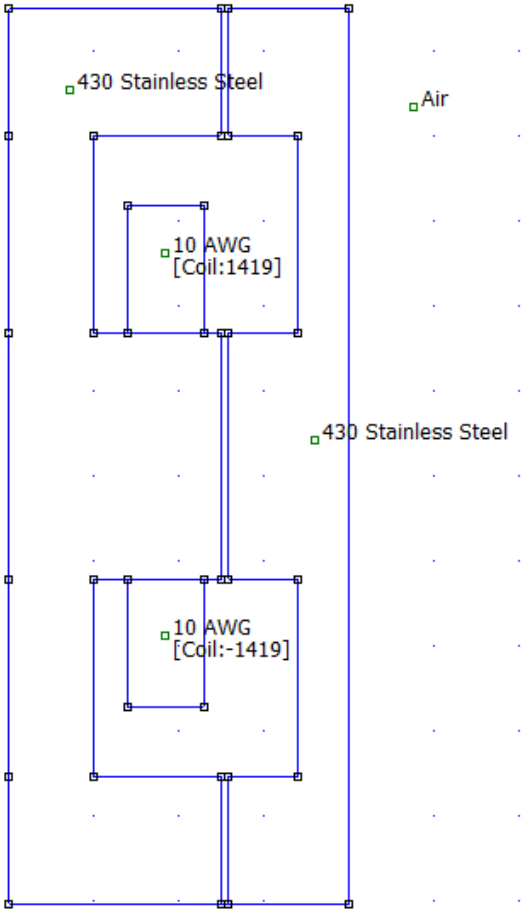

Figure 7.3 – Bonded to electromagnet materials

7.3 Creating a Model of an AC electromagnet, parameter output

Now that everything is set up, start triangulation, after which start automatic calculation. Ready model is shown on figure 7.4 and triangulated view on figure 7.5.

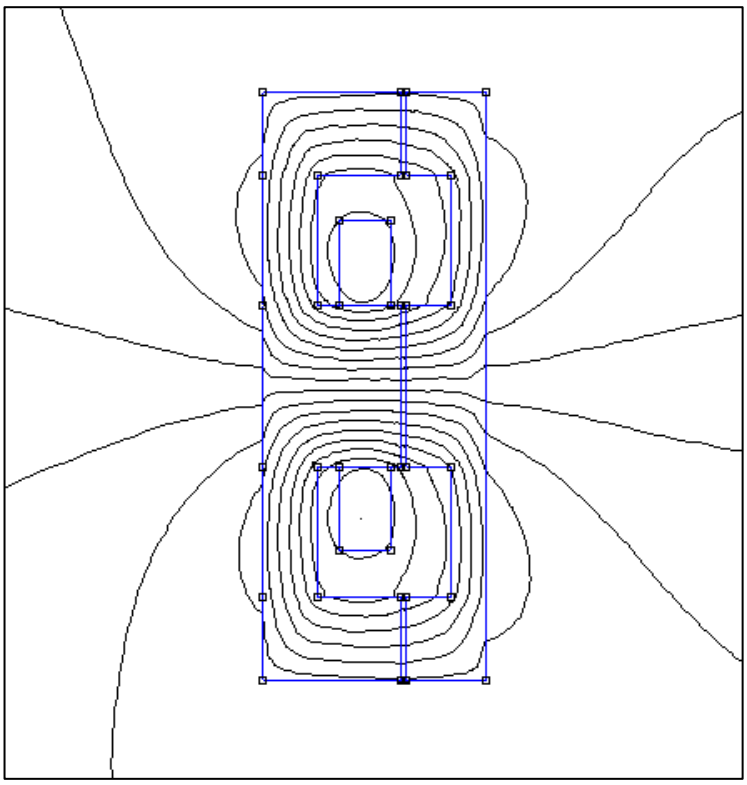

Figure 7.4 – Simulating model

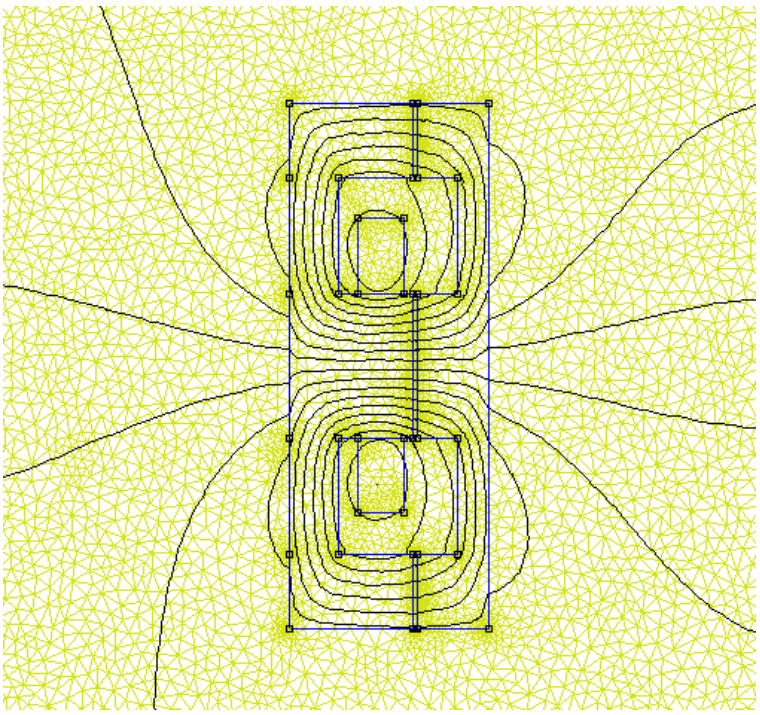

Figure 7.5 – View of mathematical model with triangulation

Open the flux density graph.

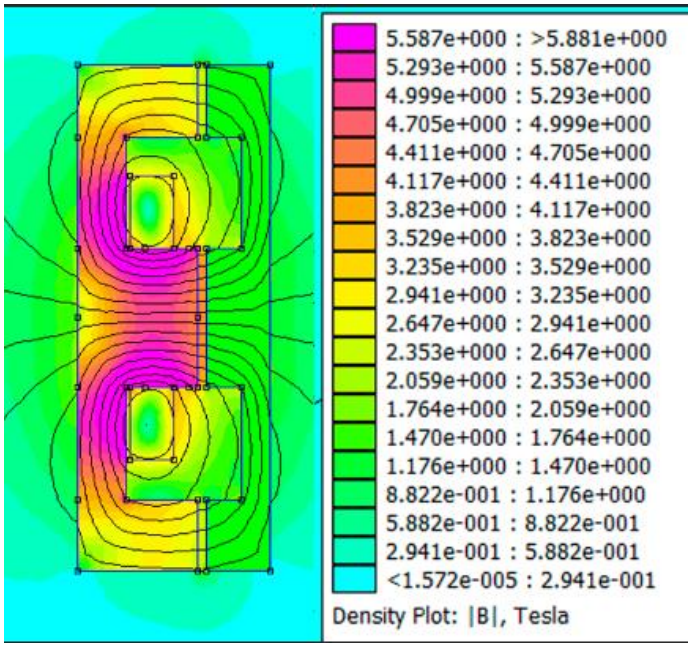

Figure 7.6 - Flux density graph.

Intergating results.

Magnetic vector potential (J):

$$\mathrm{J} = 205.929 - \mathrm{I} \cdot 0.00414392\ \mathrm{HA}^2.$$

This describes the total magnetic vector potential at a certain point. The real part ($205.929\ \mathrm{HAm}^2$.) represents the inductive behavior, while the imaginary part (0.00414392) accounts for phase shifts due to reactance.

Integral of A over selection:

$$-3.42311 \times 10^{-11} + \mathrm{I} \cdot 2.12611 \times 10^{-13}\ \mathrm{HAm}^2.$$

This is the total magnetic potential integrated over the selected area. The value is small due to the integration over a limited region, and the imaginary part indicates the phase of the magnetic field in that region.

Integral of A / selected area:

$$-1.25389 \times 10^{-5} + \mathrm{I} \cdot 7.78794 \times 10^{-10}\mathrm{HA}.$$

Magnetic field energy: 258276 J.

This is the total energy stored in the magnetic field. High energy indicates strong magnetic coupling or inductive behavior.

Hysteresis, laminated eddy of proximity effect losses: 0.650925 W.

This accounts for energy losses due to hysteresis and eddy currents. These losses occur when the magnetic field causes small circulating currents in the material, converting some energy into heat.

Resistive losses: 5306.48 W.

This is the power loss due to the resistance of the conductors, also known as I^2R losses. It indicates how much energy is being lost as heat due to the resistance of the material.

Total current: $-1.98273 \times 10^{-10} A$.

This is the net current in the system, which in this case is very small, suggesting near-equilibrium or cancellation of opposing currents.

The total volume of the selected region where the calculations are performed: 2.73×10^{-6} m^3.

Lorentz force (J x B). Steady-state force: x-component: -430.878 N; y-component: -1.39571 N; 2x frequency force: x-component: -430.878+ I · 0.115331 N; y-component: -1.39571– I · 0.000286194 N.

Force results from the interaction between the current and the magnetic field. The steady-state force represents the constant magnetic force, while the 2x frequency force includes the alternating components.

Magic field coenergy: $258276\ J$.

Coenergy is a concept related to energy in systems where magnetic fields are present. It is equal to the stored magnetic energy and indicates how much work can be done by the field.

Force via weighted stress tensor. Steady-state force: x-component: -1060.62 N; y-component: 0.150227 N.

2x Frequency force, x-component: -1060.62+ I · 0.00633525 N; y-component: $0.150227 - I \cdot 3.91539 \cdot 10^{-5}$ N.

That is another way to calculate forces using the stress tensor, providing a different perspective on the force distribution.

Torque via weighted stress tensor (about 0,0). Steady State: 50.5283 N*m. 2x Frequency: 50.5283– I · 0.000303821 N*m.

That is the twisting force that results from the magnetic field. The steady-state value shows the constant torque, while the 2x frequency value includes the oscillating part.

R^2 moment of inertia/density, it is related to the rotational inertia of the system and indicates how much resistance the object has to rotational acceleration.

$$4.76098 \times 10^{-8}\ \mathrm{m}^5.$$

Total loss density: $2.07023 \times 10^{-15}\ \frac{\mathrm{W}}{\mathrm{m}^3}$.

Table 7.1 – Circuit output.

Parameter	Value
Total current	80 A
Voltage drop	132.678 + I · 2253.37 V
Flux linkage	12916.2 – I · $5.1799 \cdot 10^{-5}$ WB
Flux/Current	161.453 – I · $6.47487 \cdot 10^{-7}$ H
Voltage/Current	1.65848 + I · 28.1671 Ohm
Real power	5307.13 W
Reactive power	90134.8 VAr
Apparent power	90290.9 VA

Linear building of graphs.

In the event that the function along the contour is discontinuous, then the quality of the graph may become worse (the construction of a field on both sides of the mathematical ferromagnet material gives different graphs for discontinuous functions). Put contour across coil to collect the data.

Graphic meanings (signs) come from sequence instructions: guidance of contour points.

Potential, the graph is shown on figure 7.7:

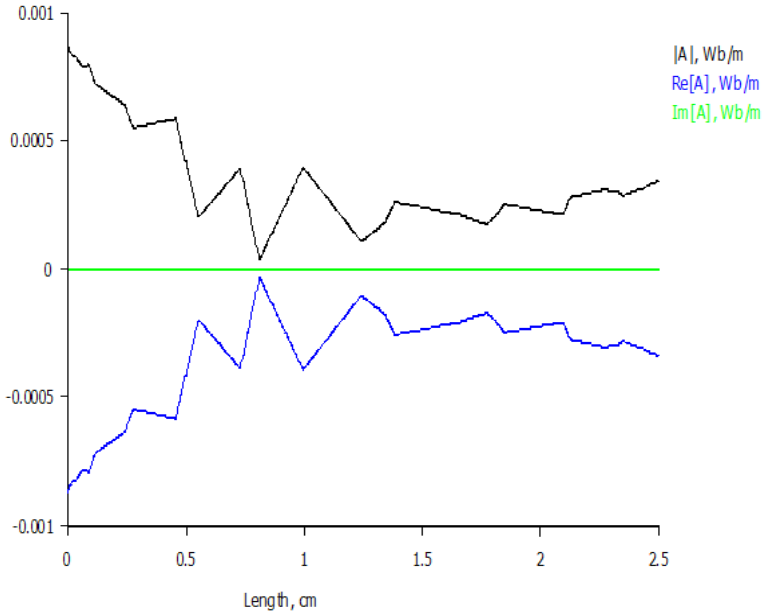

Figure 7.7 – Graph of potential in model

|B| - magnitude of flux density, the graph is shown on figure 7.8:

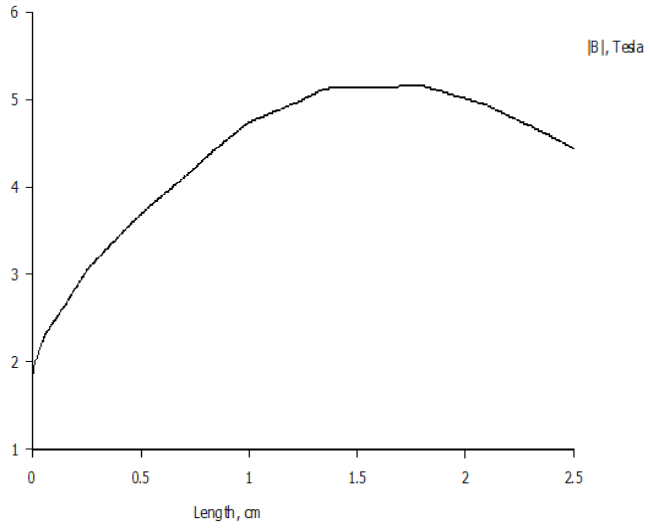

Figure 7.8 – Graph of magnitude of flux density

B. n – normal flux density, the graph is shown on figure 7.9:

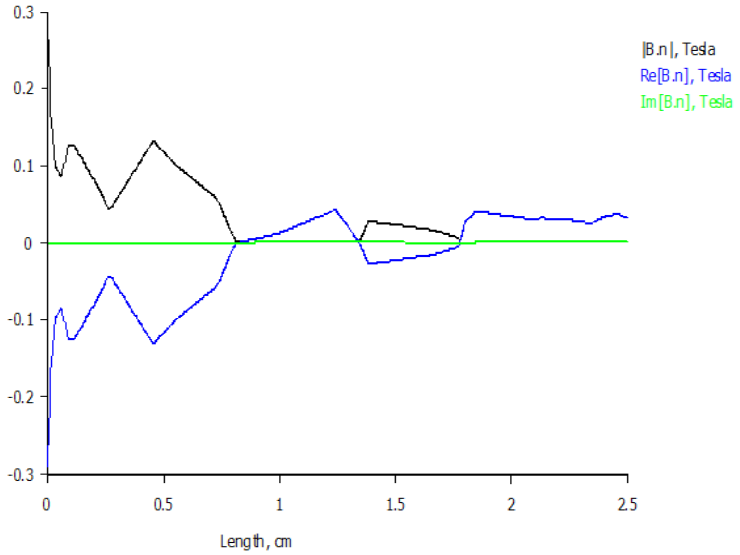

Figure 7.9 – Graph of normal flux density

B. t – tangential flux density, the graph is shown on figure 7.10:

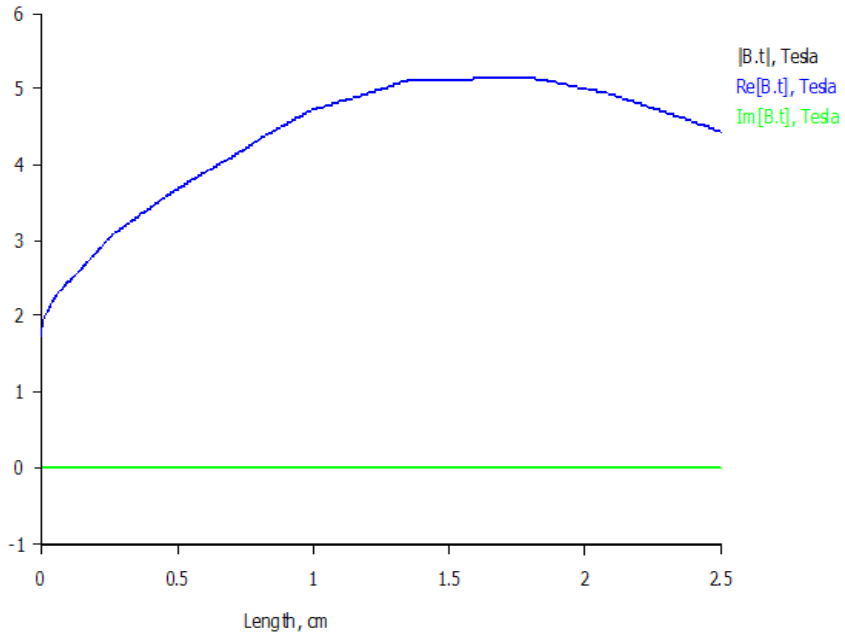

Figure 7.10 – Graph of tangential flux density

|H| - magnitude of field intensity, the graph is shown on figure 7.11:

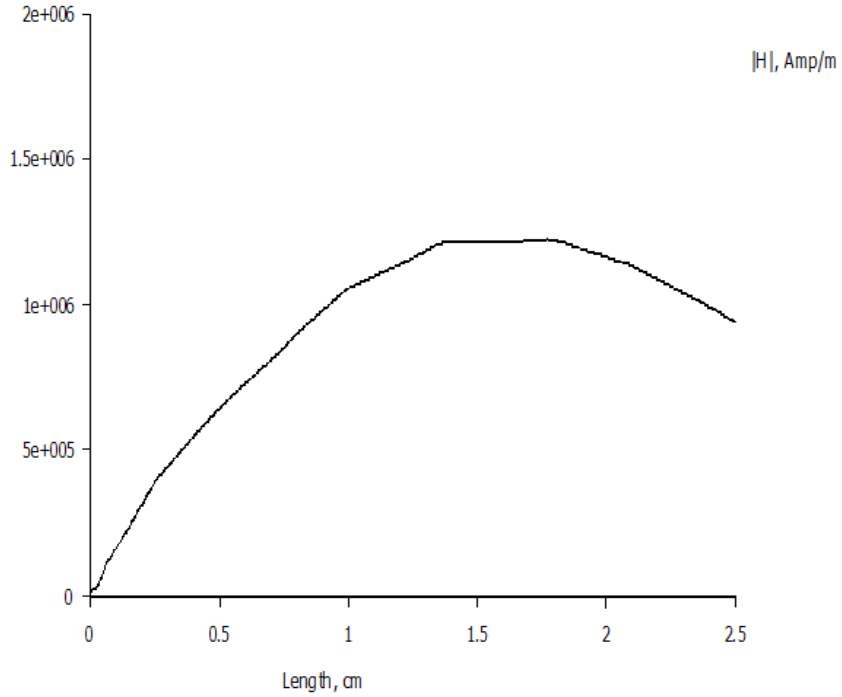

Figure 7.11 – Graph of magnitude of field intensity

H. n - normal field intensity, the graph is shown on figure 7.12:

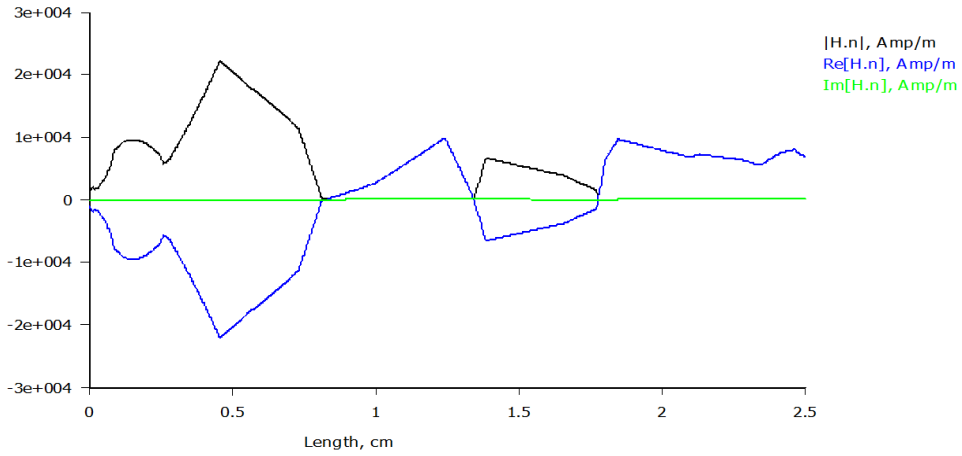

Figure 7.12 – Graph of normal field intensity

H. t - tangential field density, the graph is shown on figure 7.13:

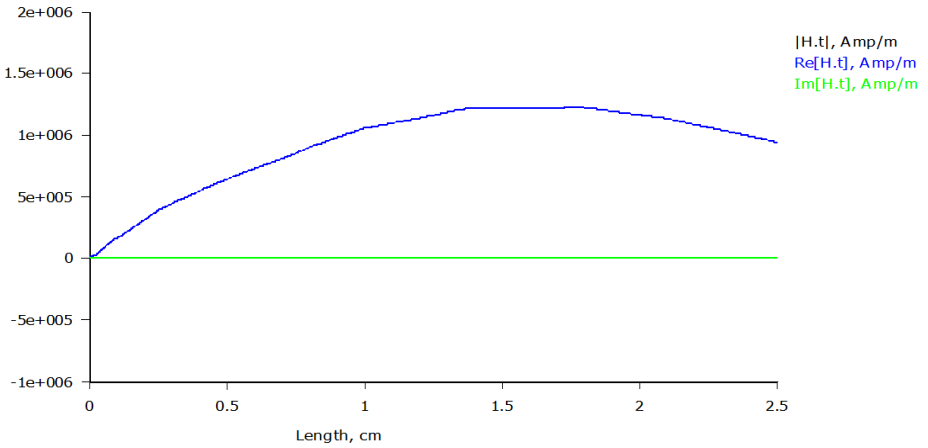

Figure 7.13 – Graph of tangential field density

J_eddy – eddy current density, the graph is shown on figure 7.14:

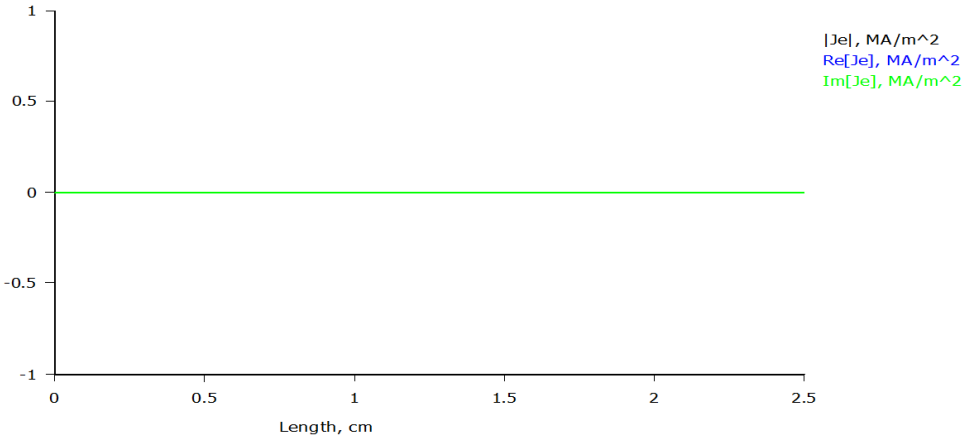

Figure 7.14 – Graph of eddy current density

Js+J_eddy – (Source+eddy+eddy_current_density), the graph is shown on figure 7.15:

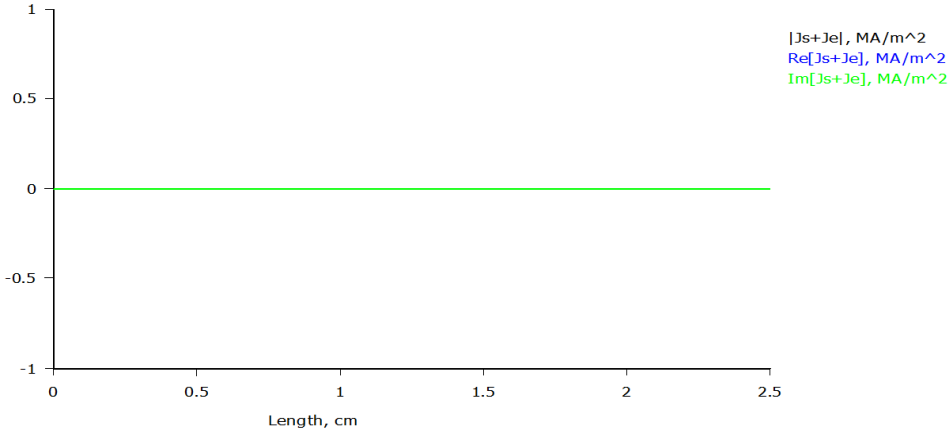

Figure 7.15 – Graph of source eddy and eddy current density

In the analysis using FEMM, several important electromagnetic parameters were calculated to assess the behavior of an AC electromagnet under various conditions. The integration results provided key insights into the system's inductance, magnetic field distribution, resistive losses, and forces acting on the components. Flux linkage and inductance showed that the system effectively stores and transfers magnetic energy, with minimal reactive components, indicating efficient performance. Magnetic energy and coenergy reflected the ability of the system to convert electrical energy into magnetic energy, crucial for optimizing the electromagnetic design. Resistive losses were quantified, allowing for adjustments to minimize energy dissipation as heat. Forces (Lorentz and stress tensor) provided insight into the mechanical effects of the magnetic field on the structure, important for ensuring stability and durability. The calculated torque and force distribution offer essential data for fine-tuning mechanical properties and preventing failures during operation.

Work with FEMM helps with it results to get better control over electromagnetic systems and it real-world model of contactor. Also it helps to optimize the design for efficiency, performance, and safety, ensuring that the electromagnet operates within safe thermal and mechanical limits.

CONCLUSION

For this project, an AC contactor with a rated current of 80 A and voltage of 380 V was designed, which served as the prototype for the contactor ПМ 4-80. Foreign analogues were also reviewed during the design process.

The assessment of the elements within the current-carrying circuit was completed, involving the choice and computation of output buses, contact connections, switching contacts, wear considerations, contact follow-through, and the design of flexible couplings. Copper was selected as the primary material for these circuit elements, while silver coverings were applied to the switching contacts to enhance thermal stability during continuous operation.

Subsequently, the apparatus mechanism was devised, encompassing calculations for opposing forces and initial electromagnetic assessments. This phase involved determining the magnetic circuit's dimensions, the magnetizing force of the winding, and their respective geometrical dimensions.

Regarding arc control, the methodology of free blowout employing two breaking points was adopted. The process involved testing the arc blowout conditions for effective arc extinguishing. Detailed design drawings of the apparatus, including its main components, were meticulously created and incorporated.

The working model was built and modulated under work conditions. Magnetic fields view and many results of working model was obtained, everything works without problems.

LIST OF REFERENCES

1. Liu, S. Condition evaluation of AC contactor based on the grey fuzzy theory / S. Liu, Y. Wang, Z. Liu, Y. Cao, S. Zhu. - Proceedings of the 2017 4th International Conference on Electric Power Equipment-Switching Technology (ICEPE-ST), Xi'an, China, 22–25 October 2017. — Режим доступу: https://ieeexplore.ieee.org/abstract/document/8188836/.

2. Sun, S. Research on the influence of vibrations on the dynamic characteristics of AC contactors based on energy analysis / S. Sun, J. Cui, T. Du. - Energies, 2020. — Режим доступу: https://www.mdpi.com/1996-1073/13/3/559.

3. Wang, G. Simulation of dynamic behavior and contact bounce of AC contactor / G. Wang, R. Yu, X. Li, H. Chen. - 2023 IEEE 68th Holm Conference on Electrical Contacts (HOLM), 2023. — Режим доступу: https://ieeexplore.ieee.org/abstract/document/10352193.

4. Yang, C. Investigation of making process and associated contact bounce behaviors for alternating current contactor / C. Yang, Z. Zheng, W. Ren. - 2021 IEEE 66th Holm Conference on Electrical Contacts (HLM), 2021. — Режим доступу: https://ieeexplore.ieee.org/abstract/document/9671183.

5. Yang, D. Novel voltage sag protection topology of contactors for uninterrupted switching capability / D. Yang, X. Gao, Z. Ma, E. Cui, H. Zhang. - IEEE Trans. Ind. Appl. 2018, 54, 3170–3178. — Режим доступу: https://ieeexplore.ieee.org/abstract/document/8331166.

6. Zong, M. Researchon the key technology of contactor electrical life test / M. Zong, Y. heng Li. - Proceedings of the 2015 18th International Conference on Electrical Machines and Systems (ICEMS), Pattaya, Thailand, 25–28 October 2015. — Режим доступу: https://ieeexplore.ieee.org/abstract/document/7385049.

7. Wu, Z. A novel residual electrical endurance prediction method for low-voltage electromagnetic alternating current contactors / Z. Wu, G. Wu, H. Huang, Y. You. - IEEE Trans. Components Packag. Manuf. Technol. 2015, 5, 465–473. — Режим доступу: https://ieeexplore.ieee.org/abstract/document/7385049.

8. Kumari, S. Reliability estimation of distribution components-Contactors / S. Kumari, P. Kumar-M, M. Muralidhar. - Proceedings of the 2016 IEEE PES Asia-Pacific Power and Energy Engineering Conference (APPEEC), Xi'an, China, 25–28 October 2016. — Режим доступу: https://ieeexplore.ieee.org/abstract/document/7779849.

9. Wu, Z. A novel breaking strategy for electrical endurance extension of electromagnetic alternating current contactors / Z. Wu, G. Wu, C. Chen, Y. Fang, L. Pan, H. Huang. - IEEE Trans. Compon. Packag. Manuf. Technol. 2016, 6, 749–756. — Режим доступу: https://ieeexplore.ieee.org/abstract/document/7458846.

10. Zheng, S. Analysis of electrical life distribution characteristics of AC contactor based on performance degradation / S. Zheng, F. Niu, K. Li, S. Huang, Z. Liu, Y. Wu. - IEEE Trans. Compon. Packag. Manuf. Technol. 2018, 8, 1604–1613. — Режим доступу: https://ieeexplore.ieee.org/abstract/document/8391702.

11. Cui, H. Convolutional neural networks for electrical endurance prediction of alternating current contactors / H. Cui, Z. Wu, G. Wu, X. Xu, Y. You, Y. Fang. - IEEE Trans. Compon. Packag. Manuf. Technol. 2019, 9, 1785–1793. — Режим доступу: https://ieeexplore.ieee.org/abstract/document/8771146.

12. Sun, S. Quantitative evaluation of electrical life of AC contactor based on initial characteristic parameters / S. Sun, Q. Wang, T. Du, J. Wang, S. Li, J. Zong. - IEEE Trans. Instrum. Meas. 2020, 70, 1–10. — Режим доступу: https://ieeexplore.ieee.org/abstract/document/9225710.

13. Li, K. Electrical performance degradation model and residual electrical life prediction for AC contactor / K. Li, C. Zhao, F. Niu, S. Zheng, Y. Duan, S. Huang, Y. Wu. - IEEE Trans. Compon. Packag. Manuf. Technol. 2020, 10, 400–417. — Режим доступу: https://ieeexplore.ieee.org/abstract/document/8959153.

14. Abirami, S. AC Contactor Electrical Health Estimator Model / S. Abirami, S. Ruthvik, M.S. Ali, R.S. Kumar, J.S. Kumar. - Proceedings of the IOP Conference Series: Materials Science and Engineering; IOP Publishing: Bristol, UK, 2021; Volume 1145, p. 012070. — Режим доступу: https://iopscience.iop.org/article/10.1088/1757-899X/1145/1/012070/meta.

15. Василега П. О. Електропривод робочих машин, підручник. - Сумський державний університет, 2022. – 290 с.

16. Braunovic, M., Myshkin, N. K., & Konchits, V. V., 2006. Electrical Contacts Fundamentals, Applications and Technology. CRC Press. - 672 p.

17. Chunikhin A.A. Electrical Devices. - Moscow: Energoatomizdat (rus), 1988.- 518 p.

18. Sakharov P.V. Design of Electrical Devices. - Moscow: Energiya (rus), 1971. - 560 p.

19. Акімов Л. В. Автоматизований електропривод: елементи, теорія, системи керування. 3000 питань для самостійного навчання та контролю знань / Л. В. Акімов, П. А. Качанов, А. Н. Черенов. - Харків: Видавництво «Підручник НТУУ «ХПІ», 2011. – 532 с.

20. Клименко, Б.В. (2012). Електричні апарати. Електромеханічна апаратура комутації, керування та захисту. Загальний курс. Навчальний посібник. Харків: вид-во НТУ "ХПІ". – 320 с.

21. Statsenko O.G. Guidelines for coursework and self-study in "Electrical

22. Devices" for full-time students in the specialty 6.092204 - "Electromechanical Equipment for power generation". - Zaporizhzhia: ZNTU, 2010. - 42 p.

23. ГОСТ 434-78 Rectangular wire and copper bars for electrical purposes. Specifications.

24. URL: http://www.abb.com/product

25. URL: http://www.energy-group-ua.com

26. URL: http://www.laborant.ru/eltech/07/1/3/37-99.htm

27. URL: http://www.forca.ru/info/spravka/kontaktory-peremennogo-toka

28. URL: https://www.acko.ua/e-store/xml_catalog/kontaktori_malogabaritni_serii_pm/22590/

29. URL: https://axiomplus.com.ua/kontaktory/product-92195/#descr

30. URL: https://luxelectro.com.ua/ru/kontaktor-siemens-sirius-3rt2-3p-25a-1nc-1no-230v-ac-vintovoj-zazhim-3-detail.html

31. ДСТУ 2848-94. Апарати електричні комутаційні. Основні поняття. Терміни та визначення.

32. ДСТУ IEC 60898-1:2005. Устаткування електричне допоміжне. Автоматичні вимикачі для захисту від надструмів побутового та аналогічного застосування.